Computers and Geotechnics 165 (2024) 105857

Contents lists available at ScienceDirect

Computers and Geotechnics

journal homepage: www.elsevier.com/locate/compgeo

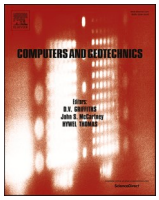

NC92Soil: A computer code for deterministic and stochastic 1D equivalent linear seismic site response analyses

Gianluca Acunzo [a], Gaetano Falcone [b,c,d,*], Annamaria di Lernia [c], Federico Mori [b], Amerigo Mendicelli [b], Giuseppe Naso [e], Dario Albarello [b,f], Massimiliano Moscatelli [b]

[a] Theta Group, Via S. Pantaleo Campano, 60/B, 00149 Rome, Italy
[b] CNR-IGAG, Istituto di Geologia Ambientale e Geoingegneria, Area della Ricerca di Roma 1, Via Salaria km 29.300, 00015 Monterotondo Stazione, Rome, Italy
[c] Department of Civil, Environmental, Land, Building Engineering and Chemistry (DICATECh), Technical University of Bari, via Orabona, 4, 70125 Bari, Italy
[d] Dipartimento di Ingegneria Civile, Edile e Ambientale, Università Degli Studi di Napoli Federico II, Via Claudio, 21, Napoli, 80125, Italy
[e] Presidenza del Consiglio dei Ministri – Dipartimento della Protezione Civile (DPC), via Vitorchiano 2, 00189 Rome, Italy
[f] Department of Physics, Earth and Environmental Sciences, University of Siena, Siena 53100, Italy

ARTICLE INFO

Keywords:
Numerical simulation
Seismic amplification
Seismic hazard
Computer-aided subsoil modelling
Open-source software
Seismic microzonation

ABSTRACT

The extensive evaluation of the impact of local seismo-stratigraphic configurations on seismic ground motion presents significant challenges due to the necessity of considering the combined effects of uncertainty and small-scale lateral variability of the relevant parameters. To effectively explore these sources of uncertainty, a new Python-based computer program is proposed for one-dimensional seismic site response simulations, adopting the equivalent linear viscoelastic approach in the frequency domain. With respect to existing software, the code introduces new pre- and post-processing features, which also meet the specific requirements of seismic microzonation studies. Within the code, the complete spectrum of uncertainties related to local seismo-stratigraphic configurations, including lithotype successions, layer thicknesses, and seismic and geotechnical properties for the considered lithotypes, is managed by considering user-defined constraints and statistical properties of the relevant parameters. Additionally, a batch approach is offered, enabling the application of the procedure to an unlimited number of different scenarios. To demonstrate the potentiality of the proposed code, a comprehensive set of 90,000 local seismic site response analyses was conducted, showing a clear correlation between the amplification factors, the mean shear wave velocity in the upper 30 m, the fundamental frequency of the deposit and the depth to the seismic bedrock.

1. Introduction

The seismic ground shaking at a given location depends on a multitude of factors. These encompass parameters associated with seismic sources and source-to-site distances (Akkar et al. 2014; Galli and Peronace 2014; Bindi et al. 2014), as well as to the local seismo-stratigraphic configurations (Gazetas 1982; Amorosi et al. 2014; Makra and Chávez-García 2016; Falcone et al. 2018; Moczo et al. 2018). In the context of Local Seismic Site Response (LSSR) analysis, where vertically propagating shear waves are of primary concern, various factors significantly influence potential amplification effects in one-dimensional (1D) configurations. These factors include the shear wave velocity profile with depth [$V_S(z)$], the soil unit weight (γ_t), the plasticity index (PI) or relative density (D_R) of soils, the non-linear (NL) soil behaviour expressed in term of constitutive equations describing secant shear stiffness [$G_S(\gamma)/G_0$] and damping ratio [$D(\gamma)$] as a function of the shear strain (γ) (Abate et al. 2007; Elia and Rouainia 2016; Dafalias and Taiebat 2016; Elia et al. 2021). Typically, LSSR analyses involve numerical simulations focused on well-investigated case studies (Makra et al. 2005; Régnier et al. 2018; Falcone et al. 2020a; Giallini et al. 2020; di Lernia et al. 2023). Several numerical codes are available for this purpose (Régnier et al. 2016; Chiaradonna 2022), such as EERA (Bardet et al. 2000), STRATA (Kottke et al. 2013), ONDA (Lo Presti et al. 2006), SCOSSA (Tropeano et al. 2016) to cite a few. Moreover, where detailed information about site conditions and mechanical behaviour of subsoil are unavailable, stochastic approaches are typically adopted (Rathje et al. 2010; Pagliaroli et al. 2014; Zalachoris and Rathje 2015; Griffiths et al. 2016; Guzel et al. 2020; Fabozzi et al. 2020). Furthermore, developing accurate subsoil models across large areas is often a formidable task due to the scarcity of laboratory and site data (Huber et al.

* Corresponding author.

https://doi.org/10.1016/j.compgeo.2023.105857
Received 27 June 2023; Received in revised form 20 September 2023; Accepted 13 October 2023
Available online 24 October 2023

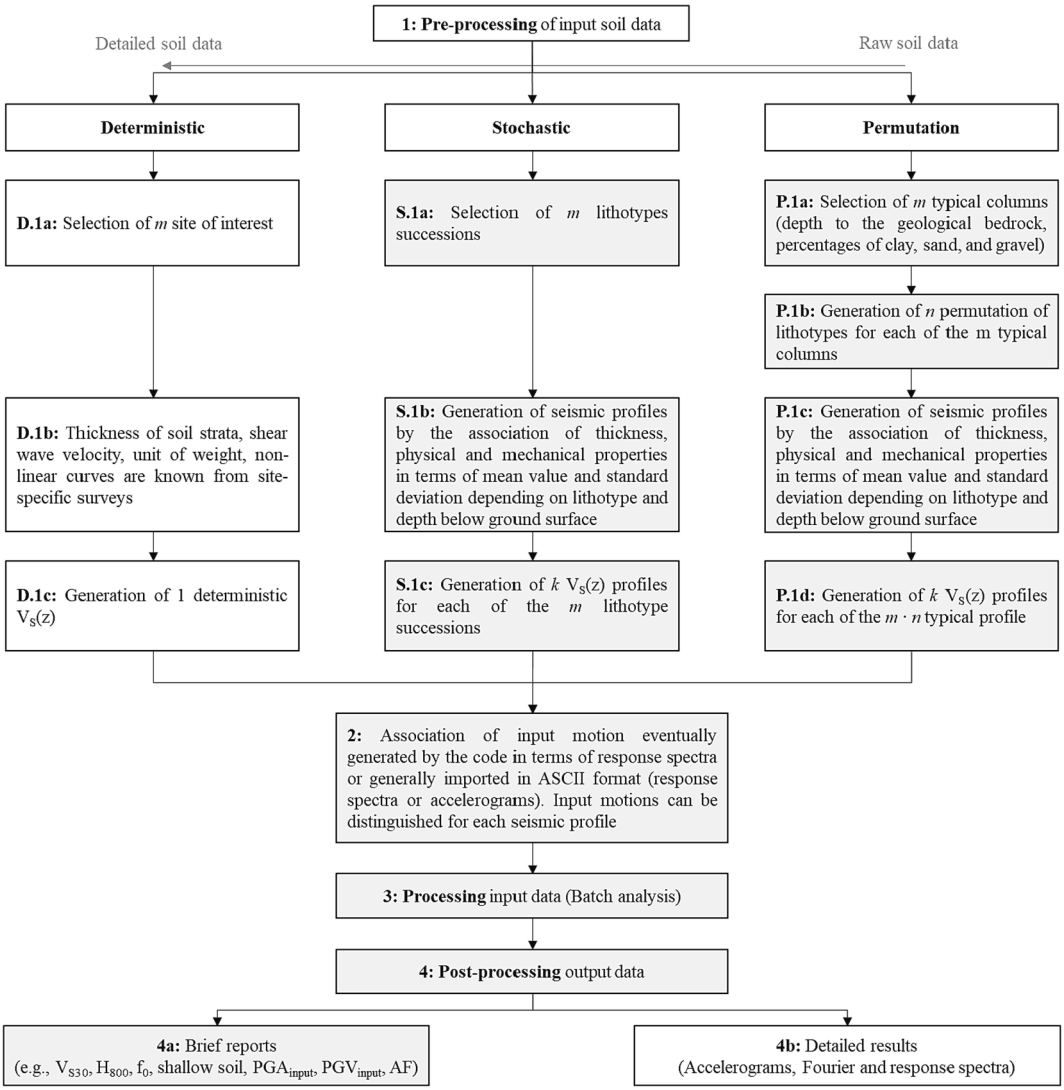

Fig. 1. Workflow of the NC92Soil computer code. Grey filled boxes refer to the improvement in the pre-processing, processing, and post-processing stages in NC92Soil code with respect to other available codes.

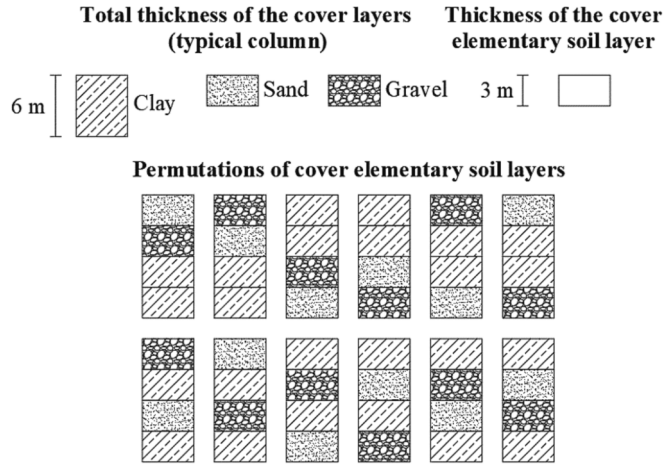

Fig. 2. Example of permutations referred to the following data: thickness of the cover deposit equal to 12 m, percentage of clay, sand, and gravel equal to 50% (6 m), 25% (3 m) and 25% (3 m), respectively, and the thickness of the elementary soil layer equal to 3 m (from Falcone et al., 2021).

2015; Mori et al. 2020b). The challenge lies in addressing the uncertainties inherent in relevant parameters, necessitating a substantial number of time-consuming analyses and post-processing efforts to produce ground shaking maps for extensive areas, as is often required in seismic microzonation studies [Working Group, 2015]. This renders manual analysis impractical to be performed. Approximate proxies (Falcone et al. 2020a) or analytical approaches are more often adopted to face this difficulty (Bindi et al. 2014; Tropeano et al. 2017; De Risi et al. 2019; Silvestri et al. 2019; Falcone et al. 2020b; Mori et al. 2020a). More effectively, several numerical codes were proposed to explore the effects of uncertainty on the input parameters by randomized simulations. Nevertheless, the available codes present some limitations when applied to typical situations of seismic microzonation studies, which require a more extensive evaluation of the relevant uncertainty. To overcome this challenge, the NC92Soil code was developed to facilitate both stochastic and deterministic LSSR analyses. Its purpose is to estimate 1D lithostratigraphic site effects for well-documented sites, as well as for case studies that rely on 'soft data' (i.e., data with less precision than hard data, but still offering potential constraints to stochastic models and applications over large areas) with a focus on seismic risk mitigation for land management. Installation files for the code are freely accessible on GitHub (Acunzo 2023). In a departure from conventional nomenclature norms, where software names often serve as descriptive

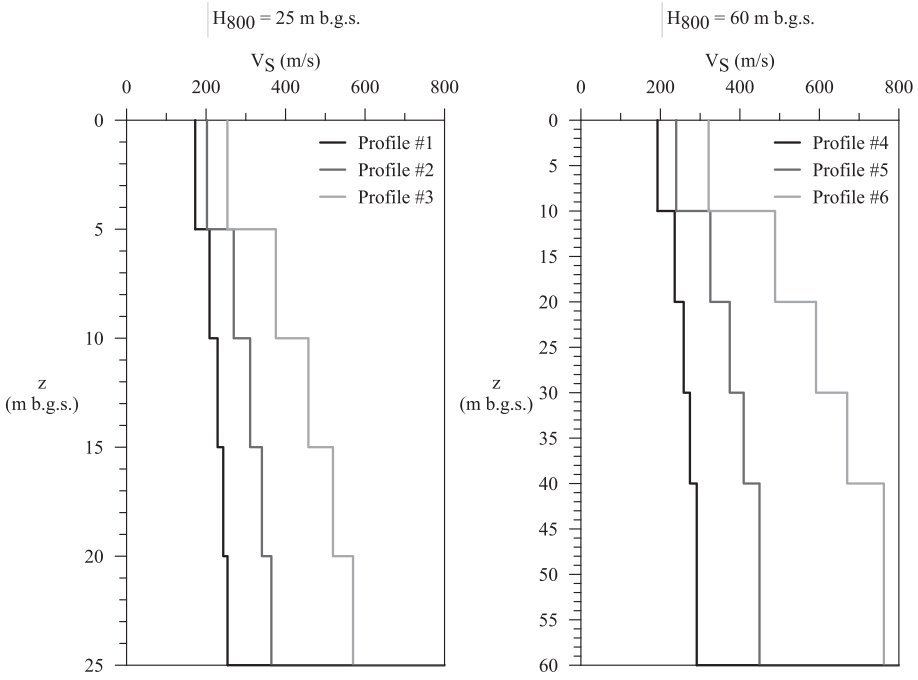

Fig. 3. The $V_S(z)$ profiles with depth adopted for the numerical simulation of LSSR by means of codes STRATA and NC92Soil.

Table 1
Correlation between γ_t, $G_S(\gamma)/G_0$ and $D(\gamma)$ curves used for the numerical LSSR analyses, and interval of depth.

z	γ_s	$G_S(\gamma)/G_0$ and $D(\gamma)$ from [39]
(m b.g.s.)	(kN/m^3)	(-)
[0, 10[	18	NL1
[10, 20[	19	NL2
[20, ∞[	19	NL3

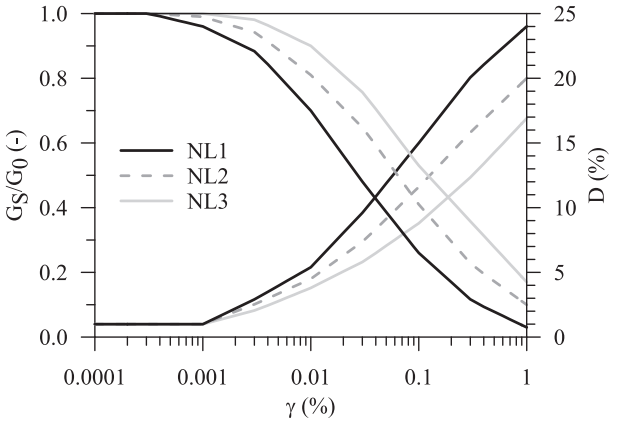

Fig. 4. Non-linear curves, $G_S(\gamma)/G_0$ and $D(\gamma)$ (Vucetic and Dobry 1991) adopted for the numerical LSSR analyses.

acronyms, in this case the name of the software was simply chosen by the authors as a veiled homage to an Italian song (Prisencolinensinainciusol by Adriano Celentano), gently reminding that also scientific endeavours can find inspiration in the most unexpected quarters.

The NC92Soil program is built upon the computational engine of STRATA (Kottke et al. 2013), known as 'PYSRA' in its Python implementation (freely available at https://github.com/arkottke/pysra). The STRATA software performs equivalent linear site response analyses in

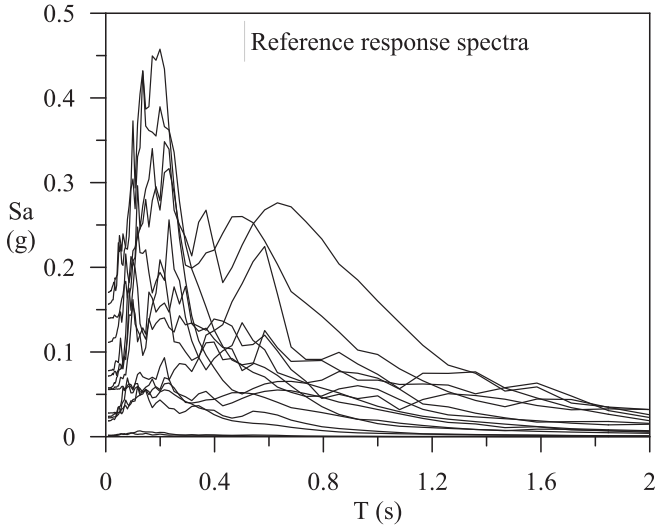

Fig. 5. Set of 15 response spectra in terms of pseudo-acceleration selected as reference outcropping motion for the numerical simulation of LSSR.

the frequency domain, adopting as input motions either acceleration time histories or response spectra based on the Random Vibration Theory (RVT) (Rathje and Ozbey 2006; Kottke and Rathje 2013). STRATA is widely adopted by researchers and practitioners and offers an approach to generate stochastic site conditions. Using these features as a foundation, extensive efforts were invested in enhancing the pre- and post-processing capabilities of the software, with the goal of also addressing the specific requirements of seismic microzonation studies (Falcone et al. 2021).

The NC92Soil code offers several functionalities, including:

- Associating physical and mechanical properties with each lithotype as a function of depth from the ground surface, based on user-defined patterns.

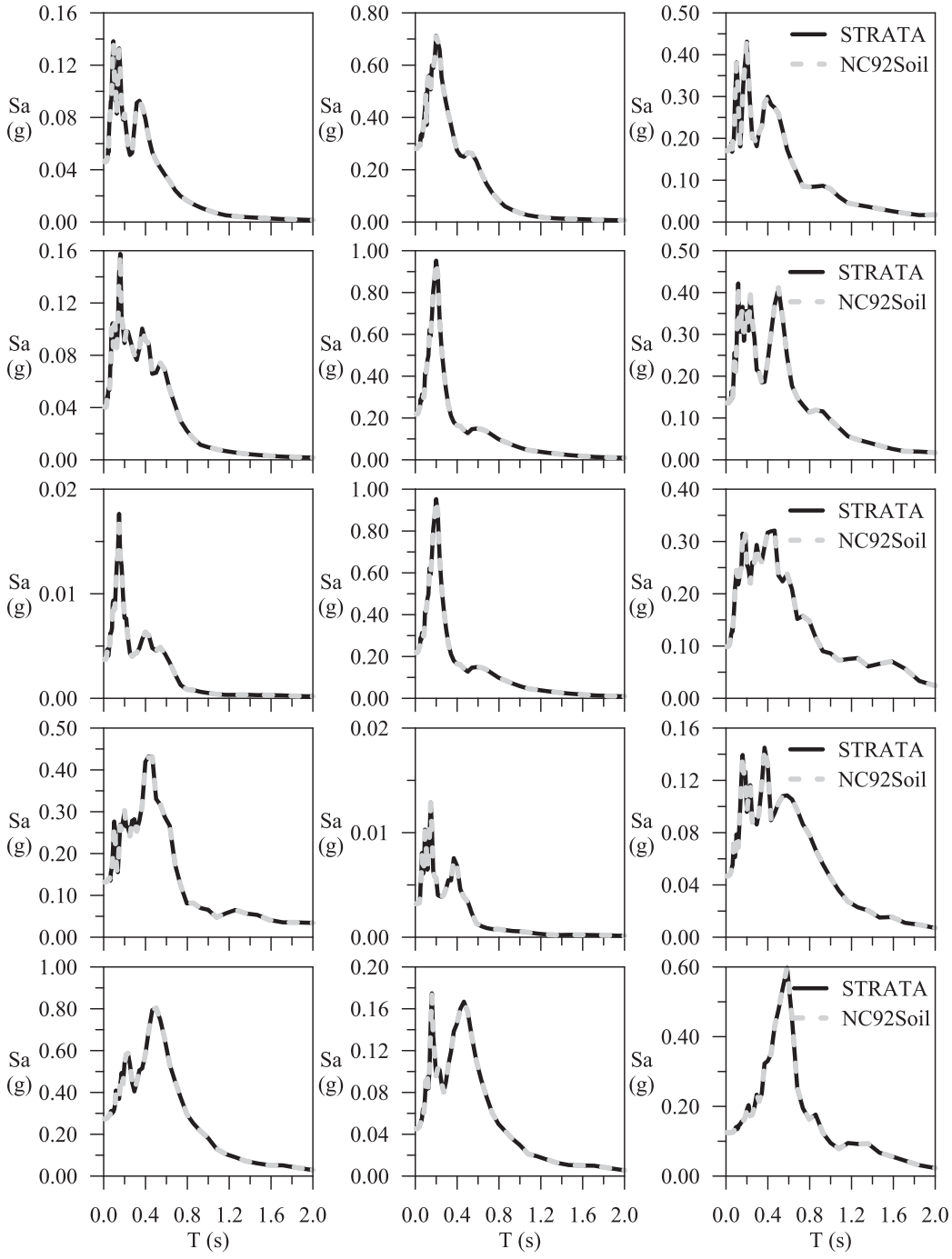

Fig. 6. Free-field response spectra obtained by means of both STRATA and NC92Soil codes with reference to profile #1 for each reference seismic motion.

- An option for batch analysis, enabling numerical simulations without user supervision.
- A stochastic approach for generating shear wave profiles variable with depth $V_S(z)$ through the Monte Carlo approach by following Kottke et al. (2013).
- The definition of lithotypes successions referred to homogeneous areas, according to the permutation approach (Falcone et al. 2021). Briefly, the permutation approach allows to generate all possible lithotype succession starting from the thickness of the cover deposit, the percentages of the cover soils (for instance, clay, sand and gravel) and the thickness of the elementary soil layer (e.g., the soil layer of which the thickness is the most common in the Italian database for seismic microzonation), which is permutated in depth.
- Quantifying amplification factors and key mechanical and geometrical parameters of analysed site profiles, ranging from one to millions.

In the following, after the description of the main features of the NC92Soil code, the testing phase is performed by comparing the results of seismic site response analyses obtained by NC92Soil and STRATA codes with reference to deterministic seismic soil profiles. Then, the capability of the code in generating stochastic seismic soil profiles is proved by comparing the 1D subsoil models obtained by both NC92Soil and STRATA codes, for target site conditions derived from Italian database of the seismic microzonation studies (DPC 2018). Lastly, in order to enlighten the potentiality of the proposed computer code, the results of 90,000 LSSR analyses are also presented. It is important to note that the intention here is not to provide a comparison of numerical results with reference to a specific real case study, as the equivalent-linear approach is well-established. Instead, the aim is to demonstrate the pre- and post-processing capabilities of NC92Soil and how data can be manipulated. Thus, the following points are addressed in this study:

- to provide insights on a new computer code for performing 1D LSSR analyses based on the linear equivalent approach in the frequency domain;
- to show the three approaches (i.e., deterministic, stochastic and permutation), which can be selected to generate the sub-soil geotechnical models and to perform LSSR analyses;
- to verify the presented code by means of the comparison of LSSR results with those obtained with the code STRATA;
- to highlight the improvements of the NC92Soil in generating sub-soil geotechnical models with respect to the available code with reference to case studies retrieved from the Italian database of seismic microzonation studies;
- to enlighten the potentiality of the code by presenting the results of 90,000 LSSR simulations aimed at identifying the correlation of ground motion amplification with soil key-factors (i.e., average shear wave velocity in the upper 30 m, V_{S30}, depth of the top of the engineering seismic bedrock, H_{800}, which is the geo-material characterised by shear wave velocity at least equal to 800 m/s, and the fundamental frequency, f_0, of the deposit) for different outcropping

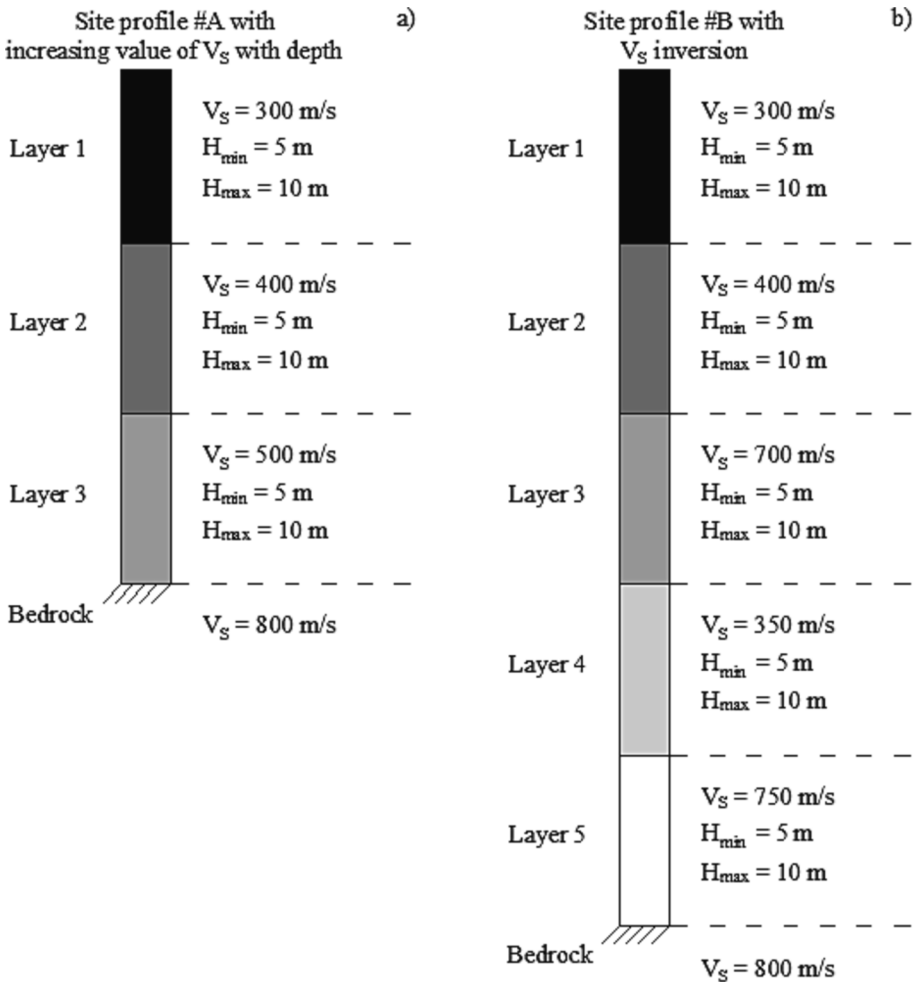

Fig. 7. Target site profiles retrieved from the Italian Database of seismic microzonation studies (DPC 2018) adopted for the comparison of the $V_S(z)$ profiles, generated by means of the Monte Carlo simulations in STRATA and NC92Soil codes. H_{min}-H_{max} is the interval over which the thickness of the layer may vary as required by the Montecarlo procedure to generate site profiles.

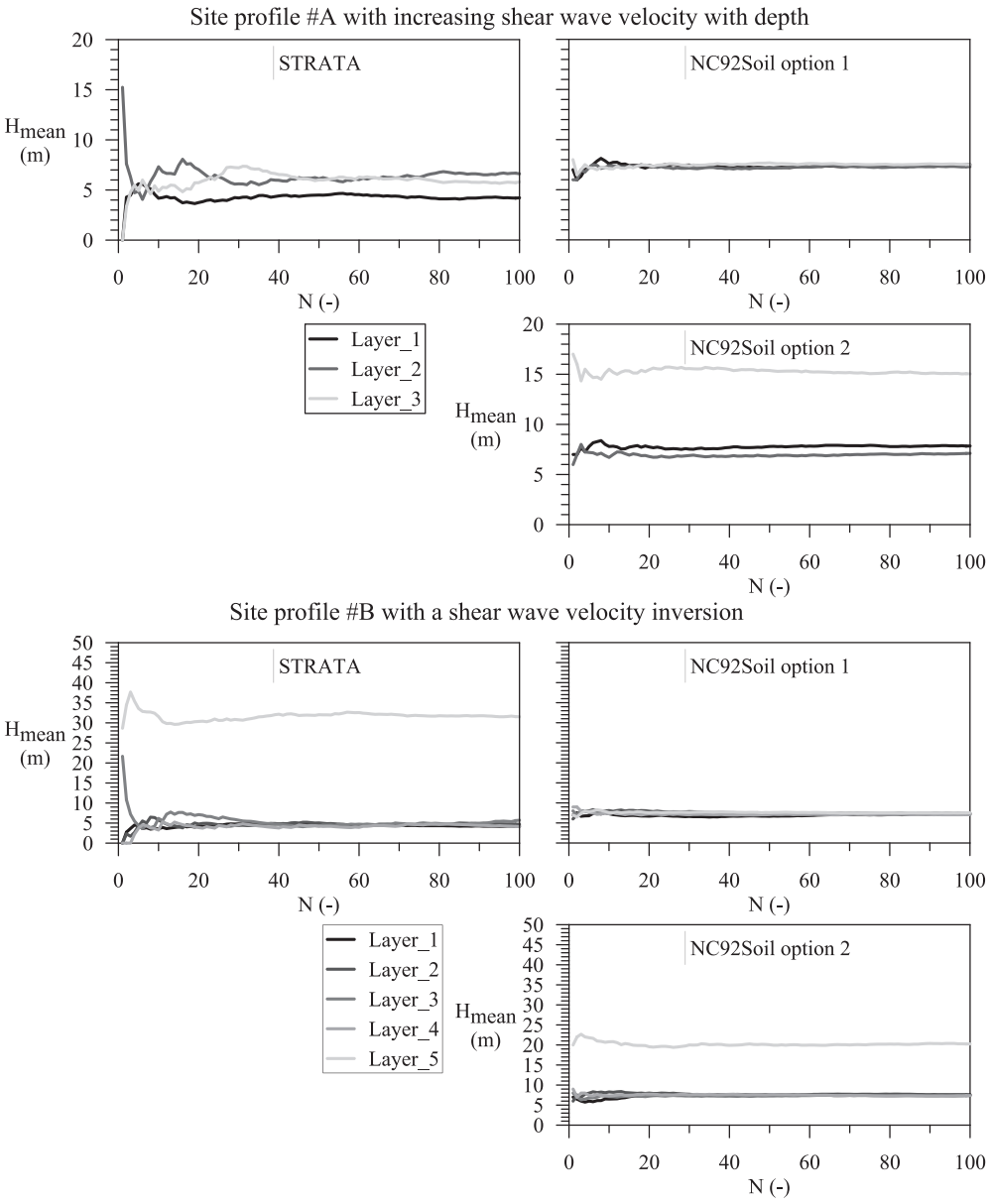

Fig. 8. Analysis of the mean value of thickness, referred to each layer, as the number of iterations N proceed in the Monte Carlo simulation.

soil lithotypes, including clay, sand, and gravel. It is worth mentioning that the case studies analysed in this paper differ from the 30 million LSSR simulations provided by Falcone et al. (2021) and Mendicelli et al. (2022). In these works, the correlation between the ground motion amplification and the V_{S30} was demonstrated with reference to the most representative site conditions across Italy.

2. Workflow of the code

The NC92Soil code is a computer program for 1D equivalent-linear site response analyses in the frequency domain, allowing for the randomization of the site properties. The code may be conceptually thought as a pre- and post- processor for the calculation engine implemented in the STRATA software.

In the pre-processing stage, the soil profiles, encompassing both the geo-lithological and the geotechnical properties, may be defined using three different approaches, i.e., deterministic, stochastic and permutation approaches (described in detail later on), according to the decreasing level of detail of the required input data. In the post-processing stage, the NC92Soil code provides results from LSSR analyses, manipulated in terms of synthetic results useful for the generation of seismic hazard maps according to the seismic microzonation standards.

Fig. 1 illustrates the workflow of the NC92Soil code, encompassing the manipulation of soil datasets (i.e., D.1a-c for the deterministic approach, S.1a-c for the stochastic approach and P.1a-d for the permutation approach) in the initial stage. Subsequently, it includes the association of input motion for each seismic profile, followed by data processing. Batch analysis can also be performed during this stage. Finally, it involves the manipulation of outputs from LSSR analyses. The grey filled boxes in Fig. 1 represent the unpublished original additional pre-processing (manipulation of soil dataset) and post-processing (manipulation of results from LSSR analysis) stages unique to NC92Soil, not available in other codes.

In the following, typical column refers to the total thickness of lithotypes down to any depth of the geological bedrock set by the user. The lithotypes succession is the soil profile defined by only topological information and lithological data for each soil layer. The seismic soil

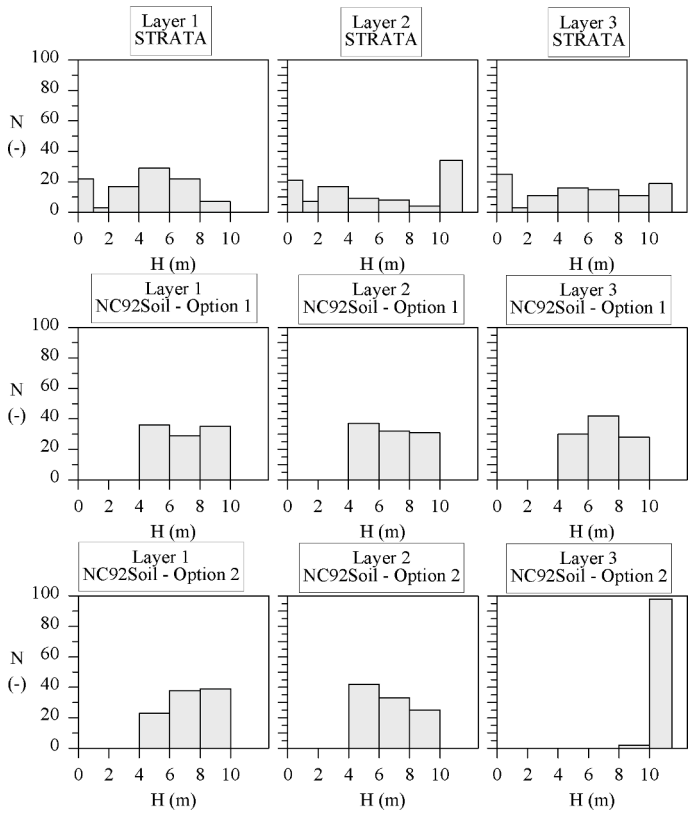

Fig. 9. Distribution of layer thickness obtained by means of STRATA and NC92soil with reference to the site profile #A characterised by increasing value of V_S with depth. NC92Soil – Option 1 and 2 are referred to the analyses performed with the bedrock extension option deactivated or activated, respectively.

dataset includes physical and mechanical parameters (i.e., V_S, $G_S(\gamma)/G_0$, $D(\gamma)$, γ_t) assigned to each lithotype within the above-mentioned lithotypes succession based on lithology and depth from the ground surface. In order to manage eventual uncertainty affecting these values, they are implemented in the form of stochastic normal or log-normal variables characterized by mean and standard deviation values. When the value is assumed to be certain, the standard deviation is null.

When the local configuration is univocally defined based on available data, the deterministic approach can be considered (i.e., steps D.1a-c, 2, 3, and 4 in the workflow) and a seismo-stratigraphical configuration is considered for computation. This results in one lithotype succession, one seismic soil dataset and one $V_S(z)$ profile.

In the other cases, two different approaches are considered to assess uncertainty affecting the expected LSSR, based on the level of accuracy of available information. When the succession of lithologies is assumed to be known, uncertainty only affects geometrical and physical parameters of the local configuration. In this case, the stochastic approach is considered to capture uncertainty affecting LSSR. Hence, variability of physical and mechanical properties with depth relative to each lithotype is considered. To this purpose, a Monte-Carlo procedure is adopted (i.e., steps S.1a-c, 2, 3, and 4 in Fig. 1) to obtain a set of *k* random configurations compatible with mean and standard deviation values representative of each parameter of the relevant lithotype (e.g., Romagnoli et al. 2022; Varone et al. 2023). Briefly, it may be considered one lithotype succession, one seismic soil dataset and *k* profiles of $V_S(z)$. Then, LSSR computations are performed relative to each configuration to obtain a population of LSSR estimates. Statistical properties of this population are considered as representative of the impact of uncertainty affecting the single input parameters on LSSR.

When the specific succession of lithotypes present in the layer stack is unknown, the permutation approach can be considered (Fig. 2). According to this approach, all the possible permutations of lithotypes (without duplicates) are generated based on the assumed respective percentage in the layer stack. In particular, each lithotype is considered to be constituted by a set of identical elementary layers. The elementary layers representative of the lithotypes are then permutated to reach the assumed bottom of the layer stack. For example, considering a total thickness of clay, sand and gravel of 6 m, 3 m and 3 m, respectively, and assuming an elementary soil layer of 3 m of thickness, a total of 12 permutations of lithotypes are generated by interchanging the positions of elementary soil layers (Fig. 2). Then, for each of these 12 lithotype succession, a set of *n* stochastic parameters configurations (i.e., $V_S(z)$ profiles) are defined by following the stochastic approach. Therefore, adopting the permutation approach (i.e., steps P.1a-d, 2, 3, and 4 in Fig. 1), more than one lithotypes succession can refer to a single typical column. Each typical column has its associated seismic soil dataset, and multiple $V_S(z)$ profiles are associated to each lithotypes successions. Consequently, for a single typical column, *n* lithotypes successions, one seismic soil dataset, *k* $V_S(z)$ profiles for each lithotypes successions are defined, resulting in a total of $n \bullet k$ $V_S(z)$ profiles.

It should be remarked that the primary innovation of the NC92Soil code lies in its capacity to perform three essential functions: *i*) permutations for the definition of the lithotype successions, *ii*) the generation of improved stochastic site profiles and *iii*) conducting several analyses using the batch analysis procedure. These advanced features, including performing batch analyses, require the prior preparation of suitable spreadsheets, by means of any either commercial or open-source software (e.g., Microsoft Excel®, Calc, Apple Numbers, etc…), to be imported within the software.

In addition to the above-described approaches, a hybrid approach might also be considered in the seismic soil profile determination. For example, in large areas, some zones may be sufficiently well-characterized to adopt the deterministic approach, while others may only have knowledge of lithological succession, requiring the stochastic approach. In such cases, detailed information about well-characterized sites should be included in a spreadsheet specifically prepared for the

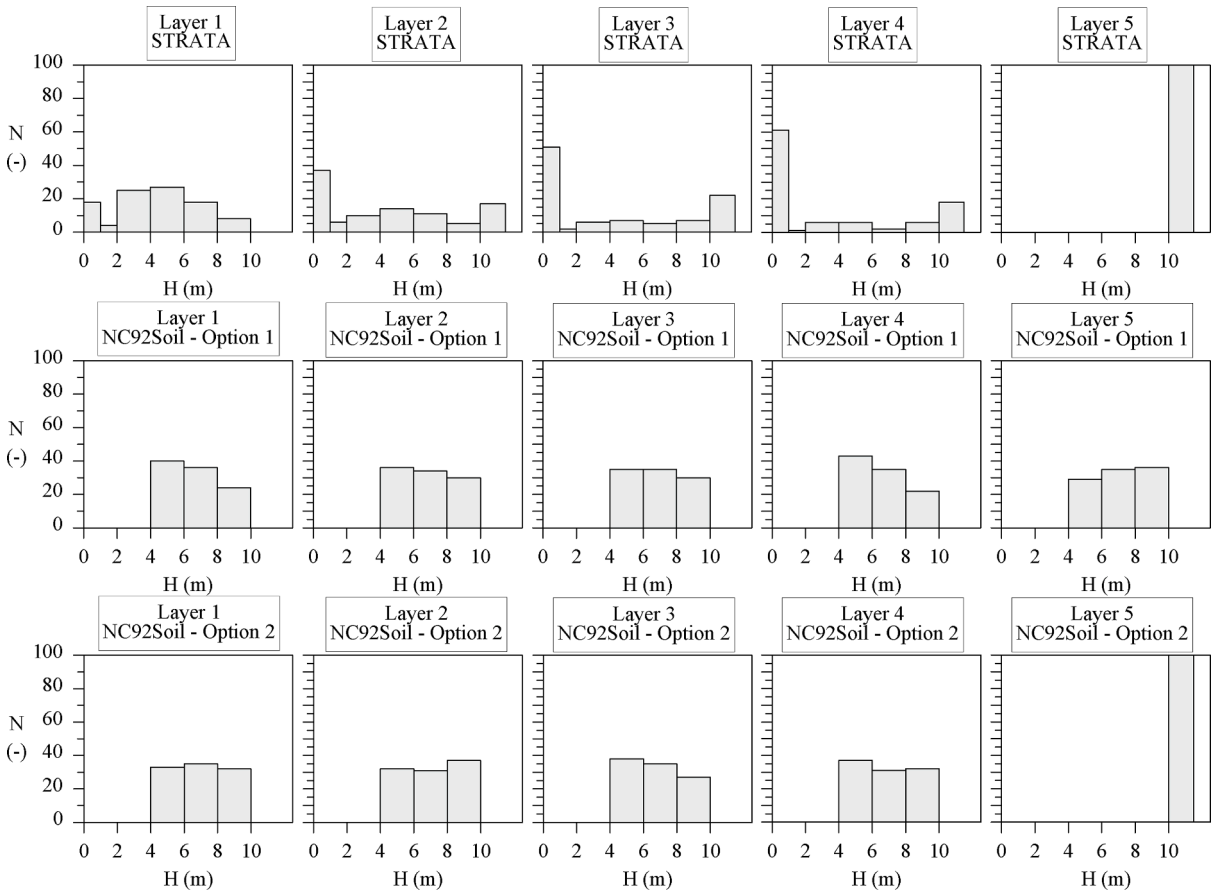

Fig. 10. Distribution of layer thickness obtained by means of STRATA and NC92soil with reference to site profile #B characterised by a V_S inversion. NC92Soil – Option 1 and 2 are referred to the analyses performed with the bedrock extension option deactivated or activated, respectively.

deterministic approach, while less detailed information for other sites in the same area of interest can be used for the stochastic determination of seismic soil profiles.

Concerning the implementation of the input motion (step 2 in the Fig. 1), the NC92Soil software allows the use of either acceleration time histories or input response spectra, the latter to be adopted with RVT (Rathje and Ozbey 2006; Kottke et al. 2013; Kottke and Rathje 2013; Chi-Miranda and Montejo 2017; Kolli and Bora 2021). In the last case, input response spectra can be either retrieved by the National Seismic hazard map (Stucchi et al. 2011) based on the coordinates of the analysed site or customized by the user. In the current implementation, the National Seismic hazard corresponds to a 475-year return period.

The output of the LSSR simulations performed through NC92Soil code are returned through both a brief report summarising synthetic results (step 4a in Fig. 1) and other spreadsheets containing detailed data, such as accelerograms, Fourier and response spectra (step 4b in Fig. 1). The synthetic results include Peak Ground Acceleration and Velocity (PGA and PGV, respectively) of the input signal, the final error of the LSSR simulation (i.e., the convergence), depth of the top of the engineering seismic bedrock (H_{800}), mean shear wave velocity referred to the numerical model of thickness H_{800} (V_{SH}), average shear wave velocity in the upper 30 m (V_{S30}), equivalent shear wave velocity (equal to V_{SH} for $H_{800} < 30$ m and V_{S30} in the case of $H_{800} \geq 30$ m), the identification name of the outcropping lithotype, the fundamental frequency (f_0), as obtained from the ratio of free-field and inside Fourier spectra, and the Amplification Factors (AF) defined by Eqs.(1)-(3).

$$AF_{PGA} = \frac{PGA_o}{PGA_i} \tag{1}$$

$$AF_{PGV} = \frac{PGV_o}{PGV_i} \tag{2}$$

$$AF_{T1-T2} = \frac{\int_{T_1}^{T_2} Sa_o dT}{\int_{T_1}^{T_2} Sa_i dT} \tag{3}$$

where Sa is the pseudo-spectral acceleration and T is the period. The subscripts *i* and *o* refer to the reference spectra (outcropping motion) and the amplified values (motion at the ground surface of the soil column), respectively. T_1 and T_2 are referred to the period intervals considered in the integral quantities, equal to 0.1–0.5 s, 0.4–0.8 s, and 0.7–1.1 s according to the guidelines for seismic microzonation (Working Group, 2015). Finally, if either permutation or stochastic approaches are adopted, NC92Soil code provides, in the brief report, additional outputs including synthetic parameter for each $V_S(z)$ profile and median and standard deviation values of the distribution of each synthetic parameter, with reference to each lithotypes succession.

3. Testing phase

With the aim of verifying the proposed code, a comparison is made between the results obtained using the NC92Soil code and those obtained with the pioneering STRATA code by Kottke et al. (2013), since both codes allow the definition of seismic soil profiles based on the stochastic Monte Carlo approach and the execution of LSSR numerical simulations based on the equivalent linear visco-elastic approach.

Firstly, the capability of the proposed code in performing equivalent linear site response analyses is assessed by comparing the results of the LSSR simulations with those generated by the STRATA code, considering

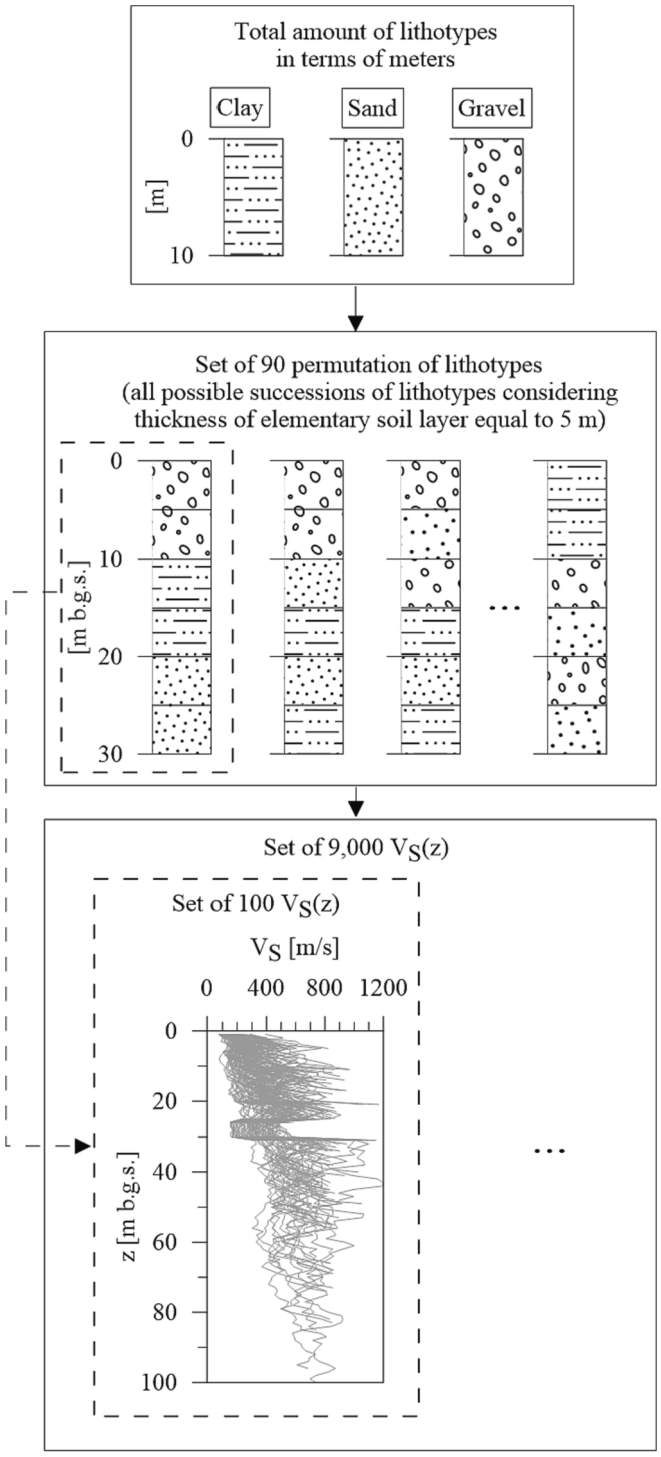

Fig. 11. Permutation workflow adopted in this study for generating 9,000 $V_S(z)$ profiles.

the same deterministic seismo-stratigraphical profiles. Secondly, the ability of the NC92Soil code in generating seismo-stratigraphical profiles through the stochastic approach is explored, focusing on two target case studies (i.e., two target site profiles) retrieved from the Italian database of seismic microzonation studies (DPC 2018). A comparison is made between the seismic soil profiles produced by the proposed code and those generated by the STRATA code, highlighting both similarities and differences between the two codes. It should be remarked that the primary distinctions arise from the fact that the STRATA code generates Vs(z) profiles in line with the recommendation given for American sites;

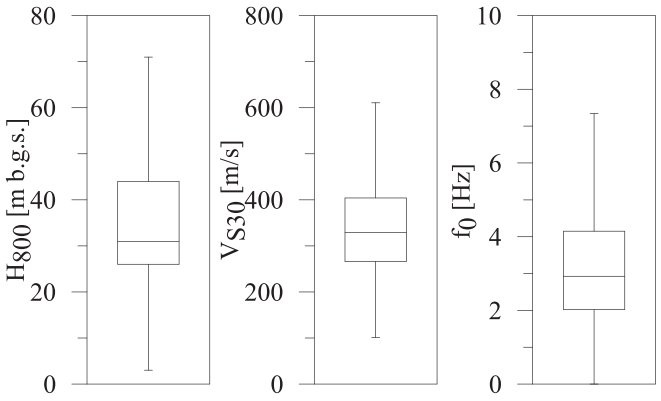

Fig. 12. Box plots of H_{800}, V_{S30}, and f_0 for the 9,000 $V_S(z)$ stochastic profiles generated by NC92Soil code.

Table 2
Main features of the reference motions selected from the Italian strong motion network for LSSR analyses.

Station ID	Component	Date	M_w	R	PGA
[-]	[-]	[-]	[-]	[km]	[g]
ACC	N	2016–10-30	6.6	18.5	0.39
ACC	E	2016–10-30	6.6	18.5	0.43
MNF	N	2016–10-30	6.6	25.1	0.12
MNF	E	2016–10-30	6.6	25.1	0.13
TERO	N	2016–10-30	6.6	46.1	0.12
TERO	E	2016–10-30	6.6	46.1	0.09
ALT	N	1980–11-23	6.9	23.4	0.06
ALT	E	1980–11-23	6.9	23.4	0.06
ANT	N	2009–04-06	6.1	26.2	0.03
ANT	E	2009–04-06	6.1	26.2	0.02

conversely, the proposed code aims at providing solutions compatible with a broad range of seismic site profile, including profiles characterised by Vs inversion, and also in agreement with the Italian requirements for the seismic microzonation studies (Santucci de Magistris et al. 2014; Hailemikael et al. 2020; Moscatelli et al. 2020).

3.1. Testing the equivalent linear approach: LSSR analyses

In this testing phase, seismic site response analyses were performed with reference to 6 deterministic $V_S(z)$ increasing with depth profiles (Fig. 3), three characterised by H_{800} equal to 25 m b.g.s. (Fig. 3a) and three characterised by H_{800} equal to 60 m b.g.s (Fig. 3b).

Depending on the depth from the ground surface, each soil layer exhibits distinct properties, including unit weight γ_t and the normalised shear stiffness modulus and the damping ratio curves, i.e. $G_S(\gamma)/G_0$ and $D(\gamma)$, as listed in Table 1. In detail, three different non-linear $G_S(\gamma)/G_0$ and $D(\gamma)$ curves (Fig. 4) were selected, representative of PI equal to 15, 20 and 30% for NL1, NL2 and NL3 curves, respectively (Vucetic and Dobry 1991). For the base of the numerical models the following parameters were adopted: $V_S = 800$ m/s, $\gamma_t = 22$ kN/m^3, $G_S(\gamma)/G_0 = 1$ and $D(\gamma) = 1\%$.

A collection of 15 reference input motions was chosen from the ITalian ACcelerometric Archive (https://itaca.mi.ingv.it/ItacaNet_30/#/home), characterised by PGA values ranging from 0.05 to 0.18 g, along with peak values of spectral acceleration pertaining to periods < 1 s. The acceleration time histories, linked to the response spectra depicted in Fig. 5, were implemented as the reference outcropping motion in both the STRATA and NC92Soil codes.

The outcomes of the numerical LSSR analyses, acquired through both codes, are compared in terms of pseudo-acceleration response spectra of the free-field motion, with reference to all the examined $V_S(z)$ profiles. To maintain conciseness, only the LSSR results for the site profile #1,

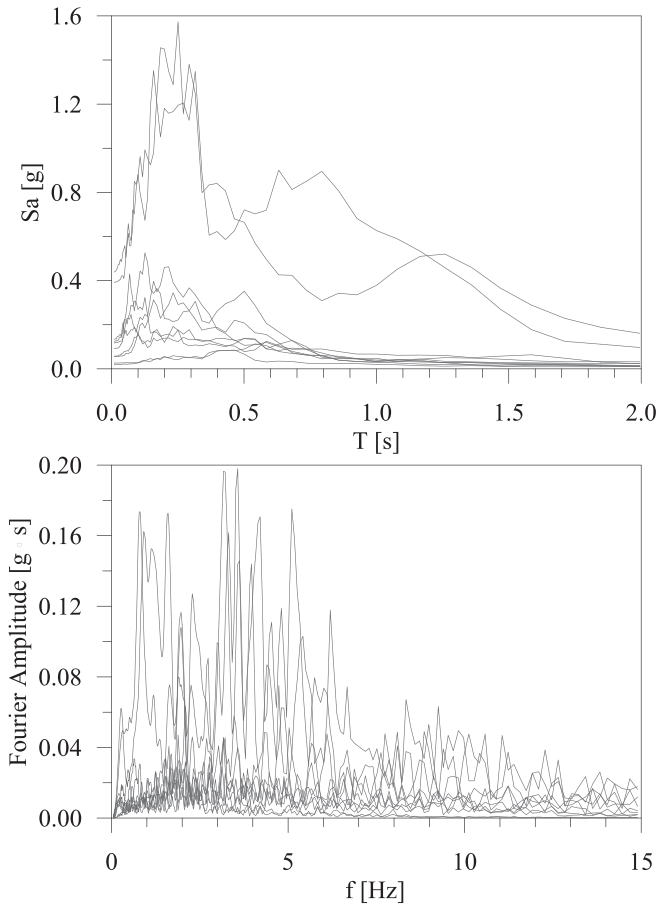

Fig. 13. Pseudo-acceleration response spectra and Fourier spectra of the 10 selected input motions.

excited by all the 15 input motions, are displayed in Fig. 6, while those referring to $V_S(z)$ profiles from #2 to #6 can be found in the Appendix A1. As expected, the results yielded by both the STRATA and NC92Soil codes exhibit strong comparability, given that the algorithm employed for equivalent linear visco-elastic analyses is identical. Additionally, the same simulations were carried out by inputting the reference outcropping motions as response spectra, in accordance with the Random Vibration Theory (RVT) approach. Also in this case, the LSSR results, not presented here for sake of brevity, exhibit strong agreement between both codes.

3.2. *Testing of the stochastic approach: generation of V_S profiles*

Two target site profiles (Fig. 7) were considered for the generation of the stochastic Vs(z) profiles through both STRATA and NC92Soil codes. The first target site profile consists of three layers with increasing value of the shear wave velocity with depth (site profile #A in Fig. 7a), while the second one is represented by a sequence of five layers characterised by a shear wave velocity inversion (site profile #B in Fig. 7b).

It is worth noting that both selected codes offer flexibility in varying the mechanical and geometrical properties of the implemented soil layers, to generate the desired numbers of $V_S(z)$ profiles consistent with the target site profile. Here, to demonstrate the efficacy of the NC92Soil pre-processing stage in creating improved seismic soil profiles, only the thickness H of the soil layers was set as a variable, keeping constant the other properties (i.e., V_S and γ_t).

Both codes enable the establishment of limits to the soil layer thickness, such as the mean value of the thickness H_{mean} of each soil layer and the range H_{min}-H_{max} over which the thickness may vary. Nevertheless, there is a distinction in approach: while STRATA models layer thicknesses as a heterogeneous Poisson process, the NC92Soil code allows separate management of each layer's thickness. Regarding the seismic bedrock, in STRATA, its depth is automatically fixed at the bottom of the implemented seismic soil profile. In contrast, the NC92Soil code provides a dual option: selecting "Option 1" automatically places the seismic bedrock at the profile's bottom, akin to STRATA. However, by opting for bedrock extension, named "Option 2", the seismic bedrock is positioned at a depth below which the time-averaged V_S exceeds 800 m/s (H_{800}). This is determined based on the V_S-z law defined for the deepest lithotype layer of the lithotypes succession (more details can be found in the NC92Soil manual and in (Falcone et al. 2021)). In this second option, it may be necessary to impose a maximum value for the seismic bedrock depth, H_{800_max}, to comply data from around the area of interest or to consider a safe condition. In the examined cases, the H_{800} maximum value, H_{800_max} was set to 30 m for the site profile #A and 50 m for the site profile #B.

A total of 100 iterations were performed through the Monte Carlo simulation to generate a total 100 different seismic soil profiles for each site profile (i.e., 1 iteration = 1seismic soil profile). Each seismic soil profile features soil layers of varying thickness, adhering to the aforementioned mean and interval thickness requirements for each layer. In general, as the number of iterations increases, the mean of the thickness H_{mean} of each soil layer tends to achieve a constant value. For the two selected case studies, 100 iterations sufficed to get stable results in terms of mean value for each layer for both numerical codes (Fig. 8). Specifically, with the STRATA code, at least 50 iterations were necessary to generate seismic soil profiles characterized by a constant H_{mean} for each soil layer, while fewer iterations were adequate to achieve stable outcomes with the NC92Soil code. In fact, the stability of the solution was attained after 20 iterations for the generation of seismic soil profiles for site profile #A, while < 20 iterations may be sufficient to get stable results for site profile #B.

The distribution of soil layers thickness as a function of the number of the generated profiles N is shown in Fig. 9 for site profile #A and Fig. 10 for site profile #B. These distributions offer insight into the quantity of seismic soil profiles among the N generated ones that possess specific soil layers with certain thicknesses H. For instance, in the case of STRATA profiles consistent to site profile #A (Fig. 8), soil layer 1 exhibits a thickness in the range [0, 1] in 22 seismic soil profiles, in the range]1, 2] in 3 seismic soil profiles, in the range]2, 4] in 17 seismic soil profiles, in the range]4, 6] in 29 seismic soil profiles, and so forth. It is worth noting that not all the STRATA profiles are consistent with the target seismic site profile #A (Fig. 9), since only 55 profiles are characterised by all the three desired layers, while the remaining 45 profiles contain at least one soil layer with a thickness of 0. Specifically, 9 STRATA profiles consist of only one layer and 36 STRATA profiles comprise two layers. This arises from the depth dependent rate model adopted in STRATA code for generating seismic soil profile consistent with American sites (Toro 1995). According to this model, the deeper the layer of interest, the greater the expected thickness for the specific layer. Conversely, all NC92Soil profiles adhere to the required characteristics of site profile #A, each featuring three soil layers of varying thicknesses.

Regarding the depth to the seismic bedrock, the STRATA profiles have H_{800} in the range of 15–30 m; for the NC92Soil profiles generated through the "Option 1", the depth of the seismic bedrock H_{800} is in the range of 16–30 m, while for those generated by means of "Option 2", H_{800} is consistently set to the user-defined H_{800_max} of 30 m, as the deepest layer has V_S = 500 m/s.

Concerning the target site profile with a V_S inversion (Fig. 10), none of the soil profiles generated by STRATA meet the required configuration for the site profile #B, which should be characterised by 5 soil layers. In detail, 25 soil profiles are composed of 3 soil layers, 59 soil profiles include just 2 soil layers and 16 soil profiles are characterised by only 1 layer. Notably, 41 STRATA profiles lack the V_S inversion.

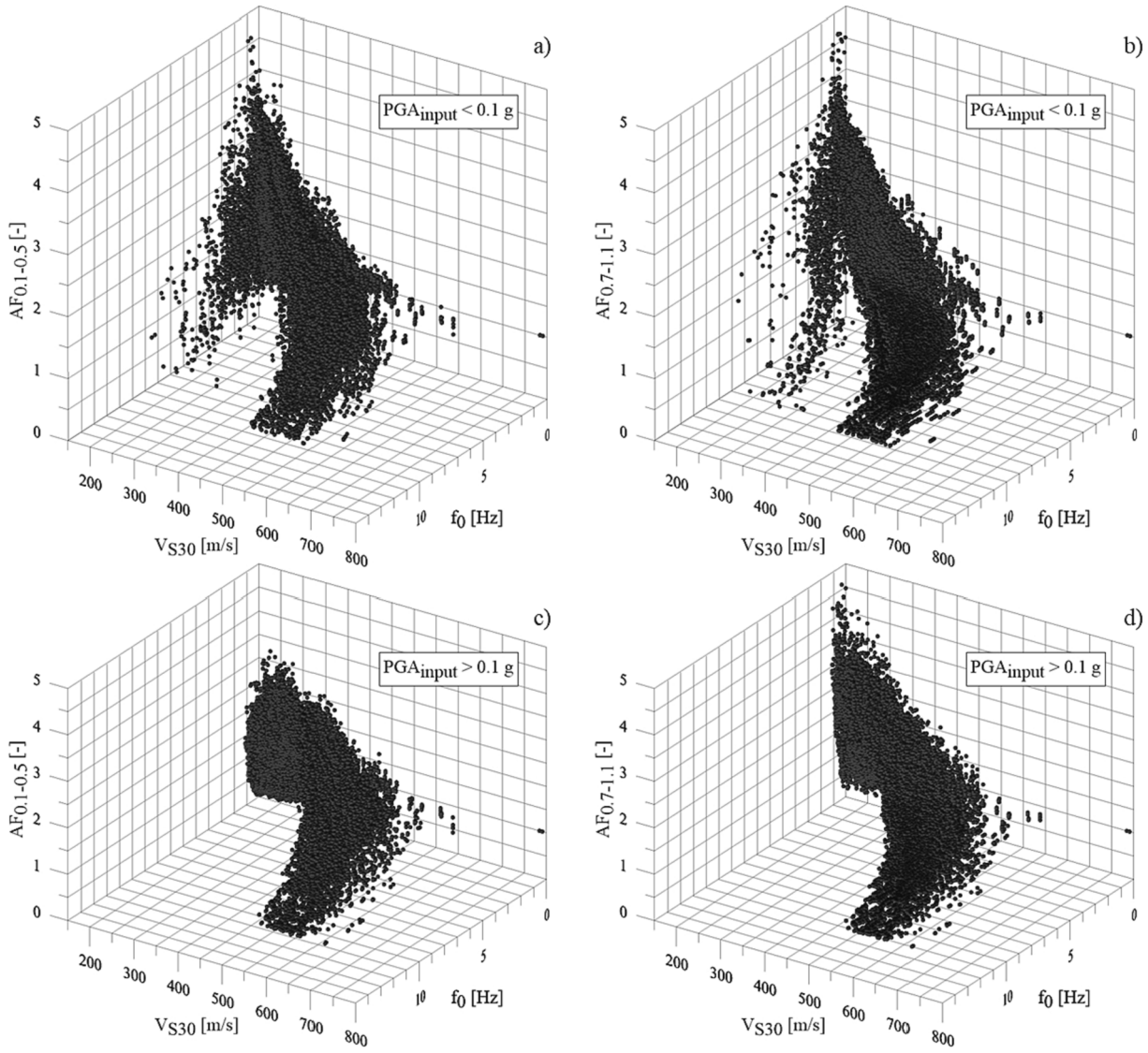

Fig. 14. Results of LSSR analyses in terms of V_{S30}, f_0, $AF_{0.1\text{-}0.5}$ and $AF_{0.7\text{-}1.1}$ differentiated for PGA of the input motion.

Conversely, the layer thickness produced by NC92Soil exhibits a uniform distribution indicated by bar charts having similar heights, regardless of the depth below the ground surface (referred to as b.g.s.), resulting in profiles that closely align with the target site profile #B.

4. The potentiality of NC92Soil code: An example of batch application

As already remarked, the key innovations of the proposed code encompass the manipulation of site data for constructing seismic soil profiles and replicating LSSR results to create maps supporting seismic risk management over extensive regions. Recently, Falcone et al. (2021) and Mendicelli et al. (2022) generated seismic amplification factor (AF) maps for Italy using the NC92Soil code. They employed site data from the Italian seismic microzonation database (DPC 2018), referred to as DB-SM, which comprises around 16,000 geophysical surveys and 44,000 continuous coring boreholes (https://www.webms.it). These data were pre-processed to create approximately 4,000 lithotype successions and 2 million $V_S(z)$ profiles. Subsequently, 15 response spectra were selected for each of the 42 homogeneous zones defined by geomorphological characteristics (normalized slope, local convexity, and surface texture (Iwahashi et al. 2018; Mori et al. 2020b)). This led to the execution of approximately 30 million LSSR analyses. The NC92Soil code was employed to process input data and results, yielding V_{S30}, input motion intensity, and AFs. These outcomes were further analysed to establish AFs-V_{S30} correlations for three categories of input motion intensity (Falcone et al. 2021; Mendicelli et al. 2022). Finally, based on maps of V_{S30} and input motion intensity for the Italian territory (Stucchi et al. 2011; Mori et al. 2020b), AFs maps covering extensive regions were generated (Falcone et al. 2021; Mendicelli et al. 2022).

It is crucial to bear in mind that for applications across vast areas, AFs need to be defined as functions of site key parameters. These parameters should exhibit strong correlations with the phenomena of interest while being readily understandable by practitioners (Zhu et al. 2020). For this reason, in this section AFs referred to 9,000 $V_S(z)$ profiles are correlated with site key-factors, notably V_{S30}, the fundamental frequency, f_0, and H_{800} among others. These factors are distinguished based on the outcropping lithotype.

The examined $V_S(z)$ profiles were generated through the permutation approach, following the steps outlined in Fig. 11. The cover lithotypes, represented by clay, sand and gravel of 10 m amount each one, were considered. Hence, the cover deposit with a thickness, H_{cover}, equal to 30 m, is underlain by cemented granular sedimentary rocks, assumed as geological bedrock. Thus, a set of 90 permutations of lithotypes were generated by interchanging the positions of elementary soil layers (i.e., layers with thickness that is most common in the database of interest),

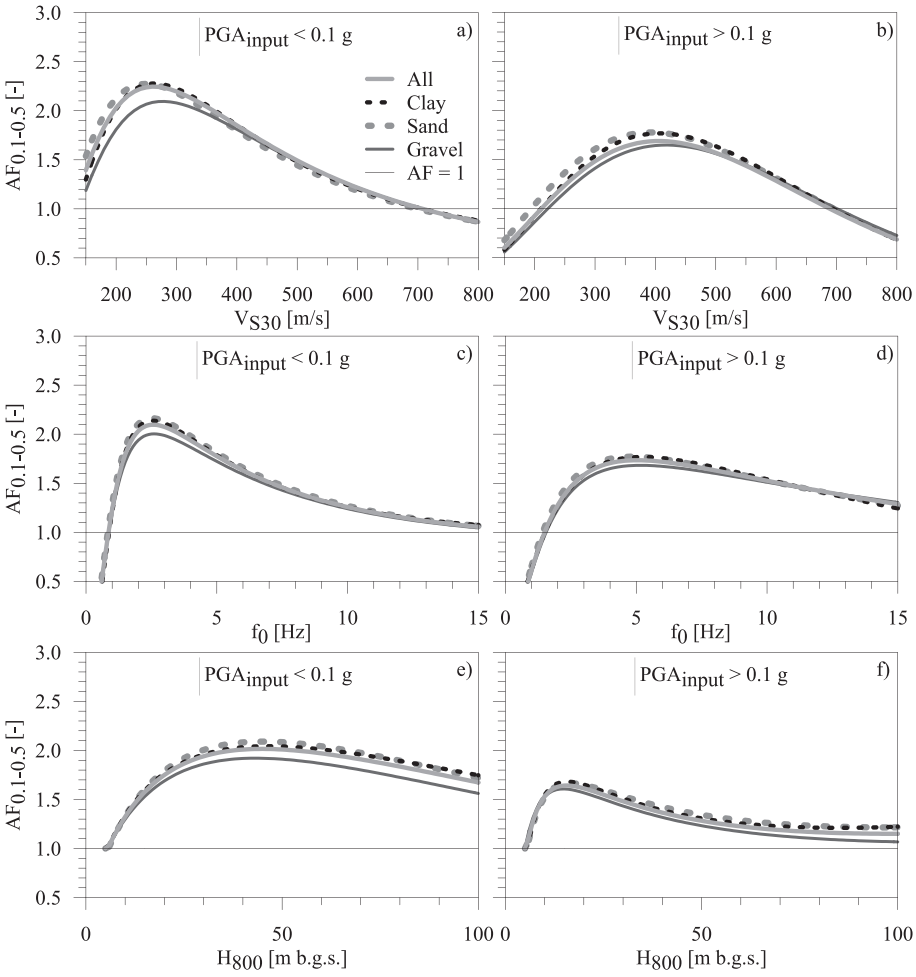

Fig. 15. $AF_{0.1\text{-}0.5}$-V_{S30}, $AF_{0.1\text{-}0.5}$-f_0 and $AF_{0.1\text{-}0.5}$-H_{800} correlations obtained by means of LSSR analyses performed using NC92Soil, differentiated for PGA of the input motion and for the outcropping material.

each assumed to be 5 m thick. For each of these 90 lithotype successions, a set of 100 stochastic $V_S(z)$ was generated, resulting in total of 9,000 $V_S(z)$ profiles to be subjected to LSSR analyses.

It is worth noting that the permutation approach was adopted to reproduce lithotypes successions from which generating stochastic $V_S(z)$ profiles extended from the ground surface down to the depth where the condition $V_S(z) = 800$ m/s is satisfied. Seismic soil profiles and $V_S(z)$ profiles were generated using physical and mechanical properties provided by Falcone et al. (2021), which are not shown herein for sake of brevity.

Fig. 12 shows the box plots of H_{800}, V_{S30}, and f_0 for the generated $V_S(z)$. Median value of H_{800} is 31 m b.g.s., while the 25th and 75th percentiles of its distribution are 26 m and 44 m b.g.s., respectively. Considering V_{S30}, median value, 25th, and 75th percentiles are 329 m/s, 266 m/s, and 404 m/s, respectively. Referring to f_0, median value, 25th, and 75th percentiles are 3 Hz, 2 Hz, and 4 Hz, respectively.

A set of 10 input motions were retrieved from the ITACA database (D'Amico et al. 2020; Nikolopoulos et al., 2022). These motions were recorded during earthquakes at accelerometric stations situated on site class A (i.e., $V_{S30} \geq 800$ m/s and flat topography). The 10 input motions were selected to represent both low and high intensity levels, in terms of PGA, and to exhibit high spectral acceleration values for periods ranging from 0.1 to 2.0 s. Specifically, 5 input motions are characterized by PGA < 0.1 g and 5 by PGA > 0.1 g. The key attributes of the reference motions selected for LSSR analyses are listed in Table 2. The Fourier spectra and pseudo-acceleration response spectra for these motions are depicted in Fig. 13. Bearing in mind that the engineering seismic bedrock were assumed to be deformable with $V_S = 800$ m/s, the reference motions were applied at the outcropping bedrock.

The results of the 90,000 LSSR analyses are shown in Fig. 14 through a 3D plot, differentiated for PGA of the input motion. The data are represented in terms of V_{S30}, f_0, $AF_{0.1\text{-}0.5}$ and $AF_{0.7\text{-}1.1}$. These results appear to exhibit significant scattering. Despite V_{S30} and f_0 serving as site key parameters and providing a synthesized representation of site conditions, closely correlating with seismic wave propagation, they alone cannot fully capture the complexity of the phenomenon. Other factors, such as the frequency content of the input motions and soil non-linearity, also play a significant role. However, there appears to be a discernible trend in the median values for both AFs-V_{S30} and AFs-f_0, which could potentially be described by Eq. (4). Furthermore, the same equation was employed to establish the AFs-H_{800} correlation.

$$AF = a \cdot x^3 + b \cdot x^2 + c \cdot x + d \tag{4}$$

where a, b, c and d represent the best-fitting parameters for the median values of the AF distribution, and x is the independent variable (i.e., V_{S30}, f_0 or H_{800} in this study).

The $AF_{0.1\text{-}0.5}$-V_{S30}, $AF_{0.1\text{-}0.5}$-f_0 and $AF_{0.1\text{-}0.5}$-H_{800} curves, as obtained fitting the LSSR results through Eq. (4), are illustrated in Fig. 15 differentiated for the input motion PGA and for the outcropping material, which could be clay, sand or gravel according to the lithotype successions. The indication of the outcropping soil may be relevant, since one could use detailed geotechnical maps for proper selecting $AF_{0.1\text{-}0.5}$-V_{S30}, $AF_{0.1\text{-}0.5}$-f_0 or $AF_{0.1\text{-}0.5}$-H_{800} curves (if surface lithology can be considered representative of the whole lithological succession).

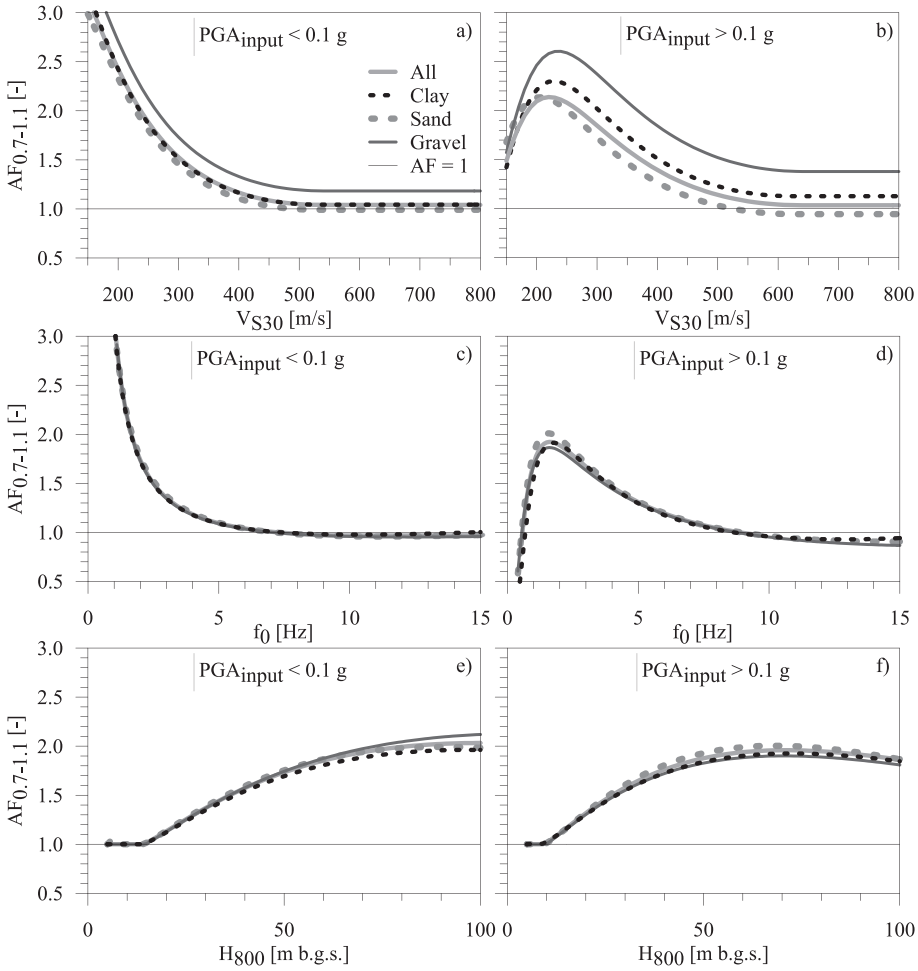

Fig. 16. $AF_{0.7\text{-}1.1}$-V_{S30}, $AF_{0.7\text{-}1.1}$-f_0 and $AF_{0.7\text{-}1.1}$-H_{800} correlations obtained by means of LSSR analyses performed using NC92Soil, differentiated for PGA of the input motion and for the outcropping material.

The $AF_{0.7\text{-}1.1}$-V_{S30}, $AF_{0.7\text{-}1.1}$-f_0 and $AF_{0.7\text{-}1.1}$-H_{800} curves are illustrated in Fig. 16**.** It should be observed that $AF_{0.1\text{-}0.5}$-V_{S30}, $AF_{0.1\text{-}0.5}$-f_0 and $AF_{0.1\text{-}0.5}$-H_{800} curves present a bell-shaped pattern, characterised by peaks at different values of either V_{S30} or f_0 or H_{800} depending on the input motion PGA. As a general observation, the curves depicted in Figs. 15-16 can be explained by considering the well-established rule $T_0 = (4 \bullet H_{800}) / V_S$, which indicates a decrease in T_0 with increasing V_S or an increase in T_0 with increasing H_{800}. For example, when $V_S = 300$ m/s and $H_{800} = 25$ m b.g.s., T_0 is 0.3 s. Consequently, the $AF_{0.1\text{-}0.5}$ peak value is expected for V_{S30} close to 300 m/s and a low PGA value in the input motion, as demonstrated in Fig. 15a. Conversely, for higher PGA values, the $AF_{0.1\text{-}0.5}$ peak value is anticipated for V_{S30} values exceeding 300 m/s, due to non-linear effects, as shown in Fig. 15b. Moreover, when $V_S = 150$ m/s and $H_{800} = 25$ m b.g.s., T_0 is 0.7 s. Accordingly, the $AF_{0.7\text{-}1.1}$ peak value is expected for V_{S30} close to 150 m/s and a low PGA value in the input motion. This does not produce a bell-shaped curve, as evidenced in Fig. 16a. Instead, for higher PGA values, the $AF_{0.7\text{-}1.1}$ peak value is projected for V_{S30} values higher than 150 m/s, due to non-linear effects that emphasize amplification at natural periods exceeding T_0, as shown in Fig. 16b. Furthermore, based on the aforementioned T_0 rule, the $AF_{0.7\text{-}1.1}$ peak value is attained for H_{800} values higher than those for $AF_{0.1\text{-}0.5}$.

Indeed, for $PGA_{input} < 0.1$ g (Fig. 15a), the maximum $AF_{0.1\text{-}0.5}$ are achieved for V_{S30} equal to about 250 m/s, while peaks of $AF_{0.1\text{-}0.5}$ are detected at about 400 m/s of V_{S30} for $PGA_{input} > 0.1$ g (Fig. 15b), irrespective of the outcropping material. Additionally, after the peaks, $AF_{0.1\text{-}0.5}$ decreases almost linearly for increasing values of V_{S30} up to 800 m/s. Moreover, for weak input motions, i.e. $PGA_{input} < 0.1$ g (Fig. 15a), the input signals are amplified for soil columns characterised by $V_{S30} < 700$ m/s, while for strong motions, i.e. $PGA_{input} > 0.1$ g (Fig. 15b), a de-amplification of the seismic motions should be expected if the soil columns are characterized by both $V_{S30} < 200$ m/s and $V_{S30} > 700$ m/s.

Similarly, the curves of $AF_{0.1\text{-}0.5}$-f_0 reach peaks at different values of f_0 for different PGA of the input motions, irrespective of the outcropping soil type. In particular, the higher the PGA_{input} the higher the f_0 at which $AF_{0.1\text{-}0.5}$ is maximum. For $PGA_{input} < 0.1$ g (Fig. 15c), $AF_{0.1\text{-}0.5}$ increases for increasing values of f_0 up to about 2 Hz and then it linearly decreases, achieving values still > 1, corresponding to amplification, for f_0 up to 15 Hz. In the same way, the $AF_{0.1\text{-}0.5}$-f_0 curves resulting for $PGA_{input} > 0.1$ g (Fig. 15d) present peaks for f_0 equal to 4 Hz, after which it decreases almost linearly. In addition, for weak earthquakes, the amplification of the seismic motion is obtained for f_0 higher than 1 Hz, while for the $PGA_{input} > 0.1$ g cases the fundamental frequency f_0 at which the seismic motion is amplified is about 2 Hz.

$AF_{0.1\text{-}0.5}$-H_{800} curves exhibit trends similar to those described above, peaking at H_{800} of 30–40 m b.g.s. and 10–20 m b.g.s. for PGA values below and above 0.1 g, respectively. Moreover, it is crucial to emphasize that $AF_{0.1\text{-}0.5}$ values are not available for H_{800} values below 5 m (Fig. 15e and f). This limitation arises because 5 m represents the minimum thickness of the soft deposit overlying the seismic bedrock within the selected case studies. Nonetheless, in scenarios where an exceedingly thin layer of soft deposit overlays the seismic bedrock, and particularly in cases lacking such a soft deposit, the reference motion should remain unaltered.

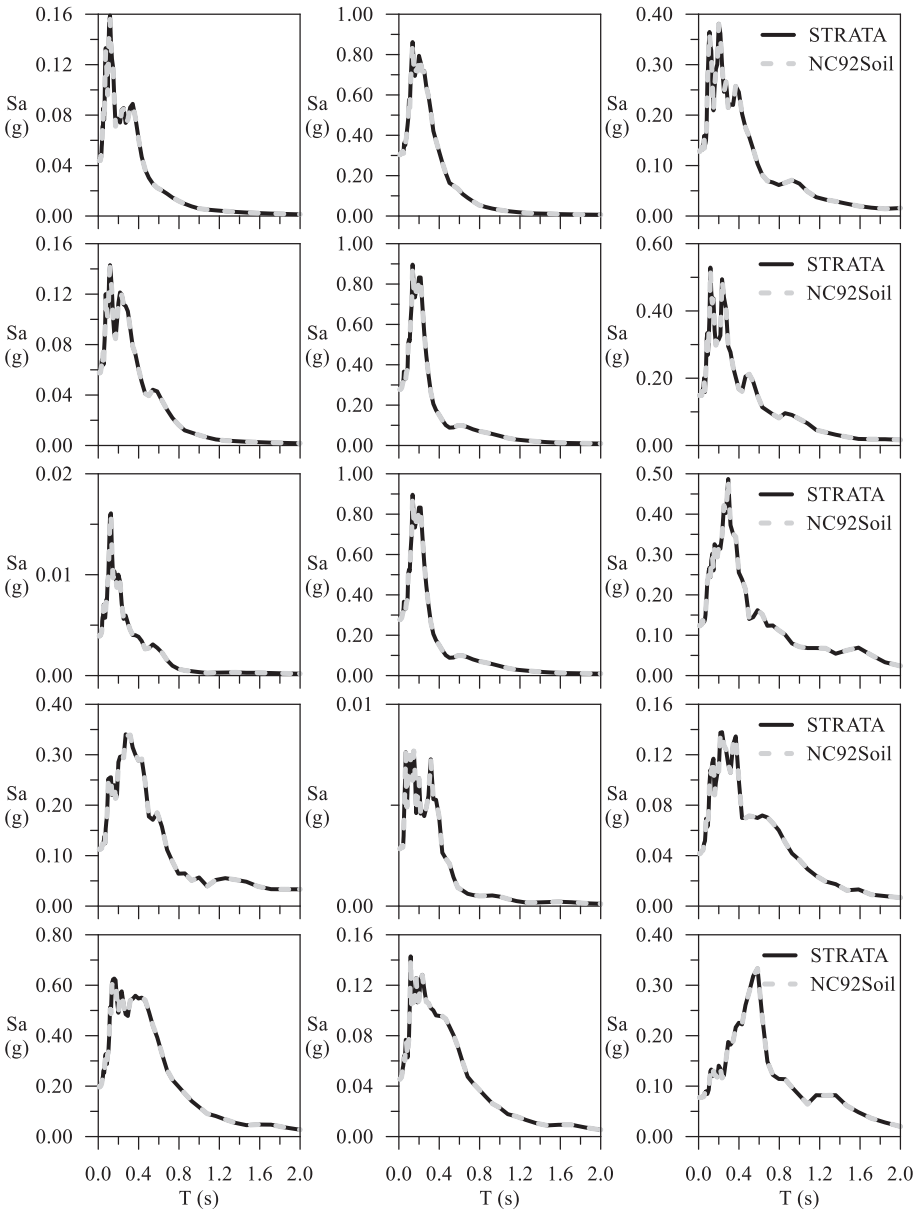

Fig. A1. Free-field response spectra obtained by means of codes STRATA and NC92Soil with reference to profile #2.

Moreover, although a strong dependence of the $AF_{0.1\text{-}0.5}$-V_{S30}, $AF_{0.1\text{-}0.5}$-f_0 and $AF_{0.1\text{-}0.5}$-H_{800} curves on the outcropping soil layer might not be detected, it could be recognised that the lowest seismic amplification could be expected when the gravel layer outcrops, since the corresponding peaks are lower than those pertaining to curves for outcropping sand and clay layers.

For completeness, the correlation curves between V_{S30}, f_0, H_{800} and the amplification factors over the larger periods $AF_{0.7\text{-}1.1}$ are also shown in Fig. 16, giving evidence to a different behaviour depending on the intensity of the input motion. Indeed, both $AF_{0.7\text{-}1.1}$-V_{S30} and $AF_{0.7\text{-}1.1}$-f_0 curves show a nonlinearly decreasing trend for increasing values of both V_{S30} and f_0 (Fig. 16a and c), when the soil columns are excited by earthquakes with PGA lower than 0.1 g. These curves reveal a tendency of the soil columns to always amplify the seismic motion, independently of the values of V_{S30} and f_0. In particular, the lower the V_{S30} or f_0 the higher the $AF_{0.7\text{-}1.1}$. Conversely, for PGA > 0.1 g a bell-shaped curve is obtained both for $AF_{0.7\text{-}1.1}$-V_{S30} and $AF_{0.7\text{-}1.1}$-f_0 correlations (Fig. 16b and d). In particular, $AF_{0.7\text{-}1.1}$ increases by decreasing V_{S30} from 800 m/s to about 200 m/s (Fig. 16b) or decreasing f_0 from higher f_0 to about 1.5 Hz (Fig. 16d). Differently from what observed for the $AF_{0.1\text{-}0.5}$ curves (Fig. 15), in this case the outcropping lithotype strongly affects the trends of $AF_{0.7\text{-}1.1}$-V_{S30} curves for PGA higher than 0.1 g (Fig. 16b), providing higher amplification factors in the case of gravel outcropping layer. In this case, given that the gravels are generally characterised by V_S higher than sands and clays (Romagnoli et al. 2022), a V_S profile with an inversion might be expected, which affect the seismic motion amplification providing amplification factors over large periods higher than those obtained in the case of V_S increasing with depth. Moreover, concerning PGA values below 0.1 g, the $AF_{0.7\text{-}1.1}$-H_{800} curves show increasing amplification with higher H_{800} values. Conversely, for PGA values>0.1 g, the peak value of AF appears to be achieved at an H_{800} depth of approximately 70 m b.g.s.

Finally, it is worth noting that different equation could be selected for fitting the results or different approaches could be adopted for predicting AF depending on site key-parameters. Finding the AF-key-parameters trends that provides the best performance is out of the scope of this study, which aims to suggest a set of possible results as retrieved from NC92Soil. Thus, the set of 9,000 stochastic $V_S(z)$ and the

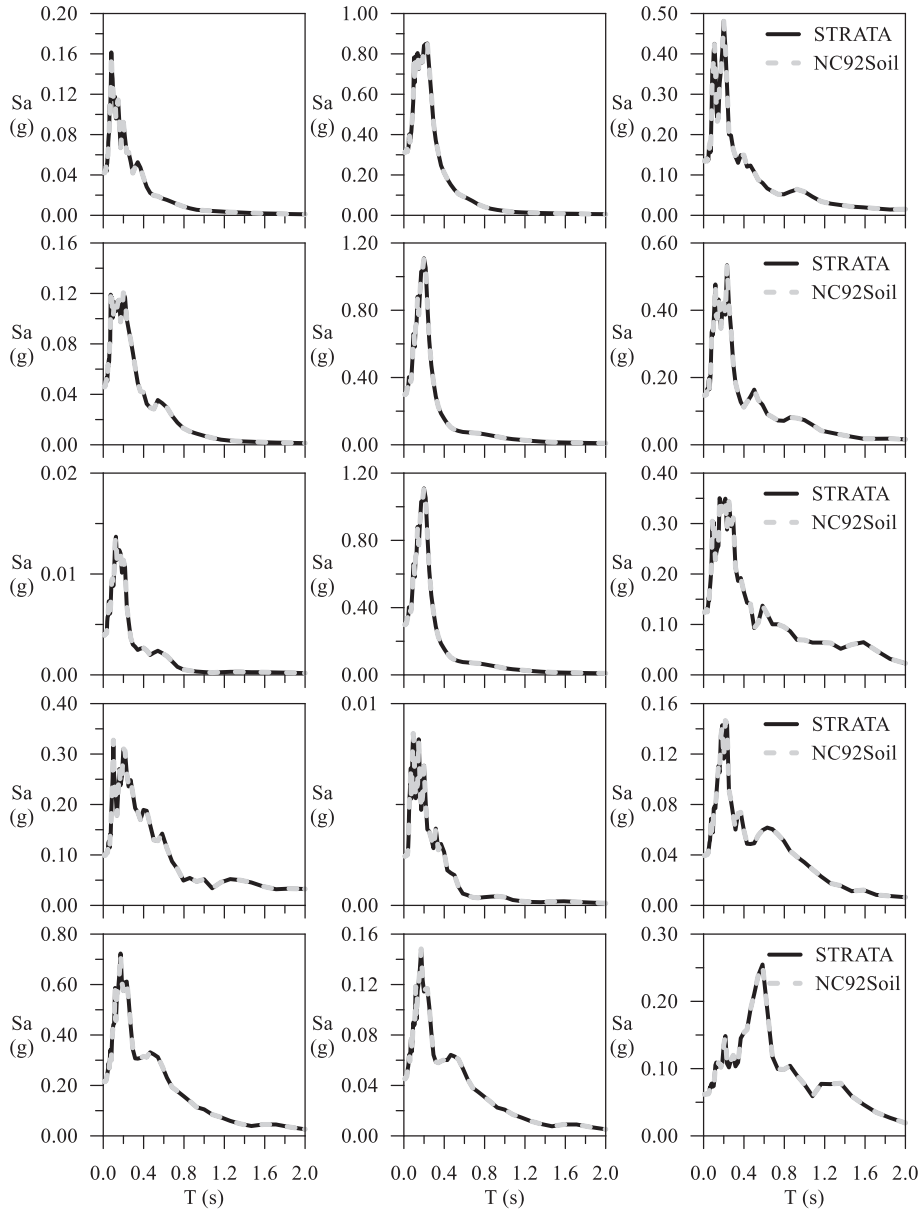

Fig. A2. Free-field response spectra obtained by means of codes STRATA and NC92Soil with reference to profile #3.

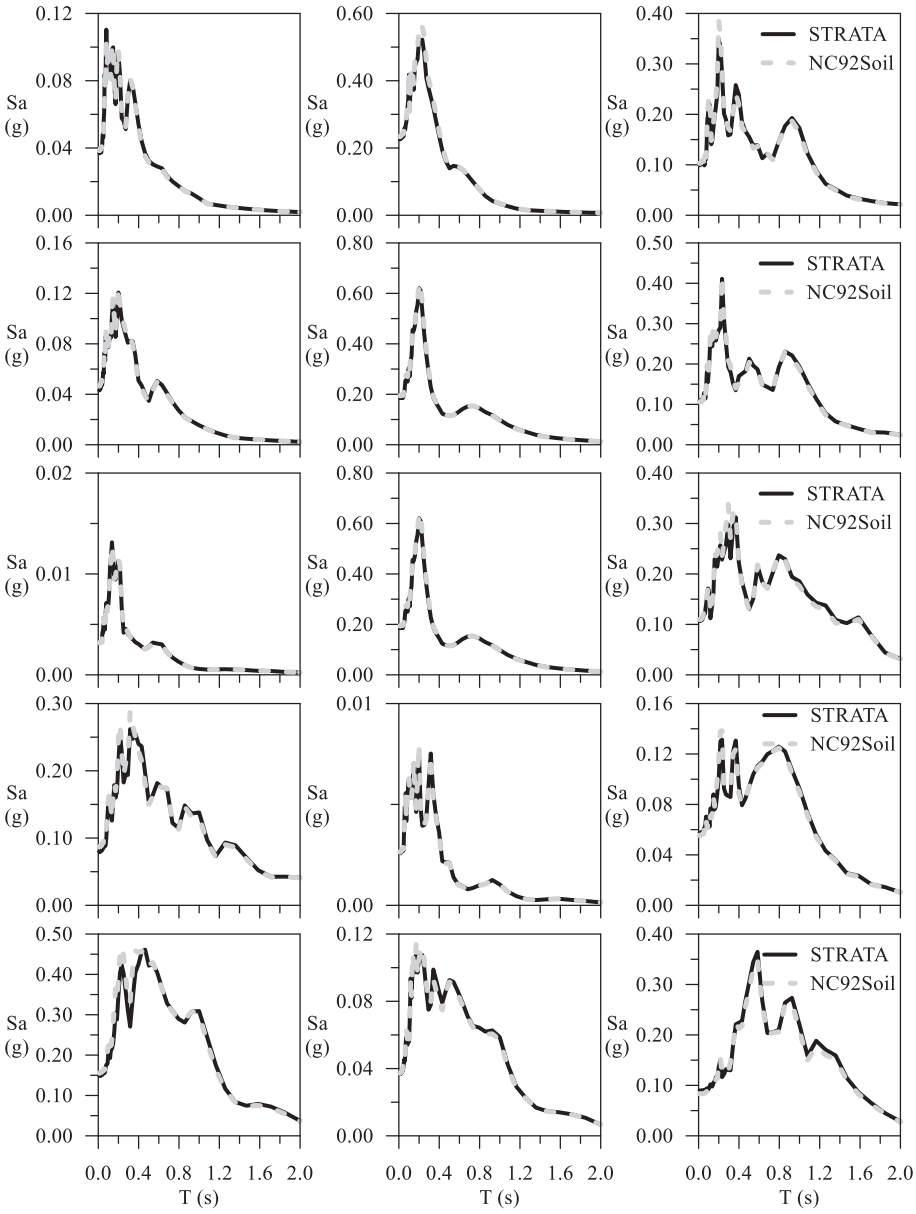

Fig. A3. Free-field response spectra obtained by means of codes STRATA and NC92Soil with reference to profile #4.

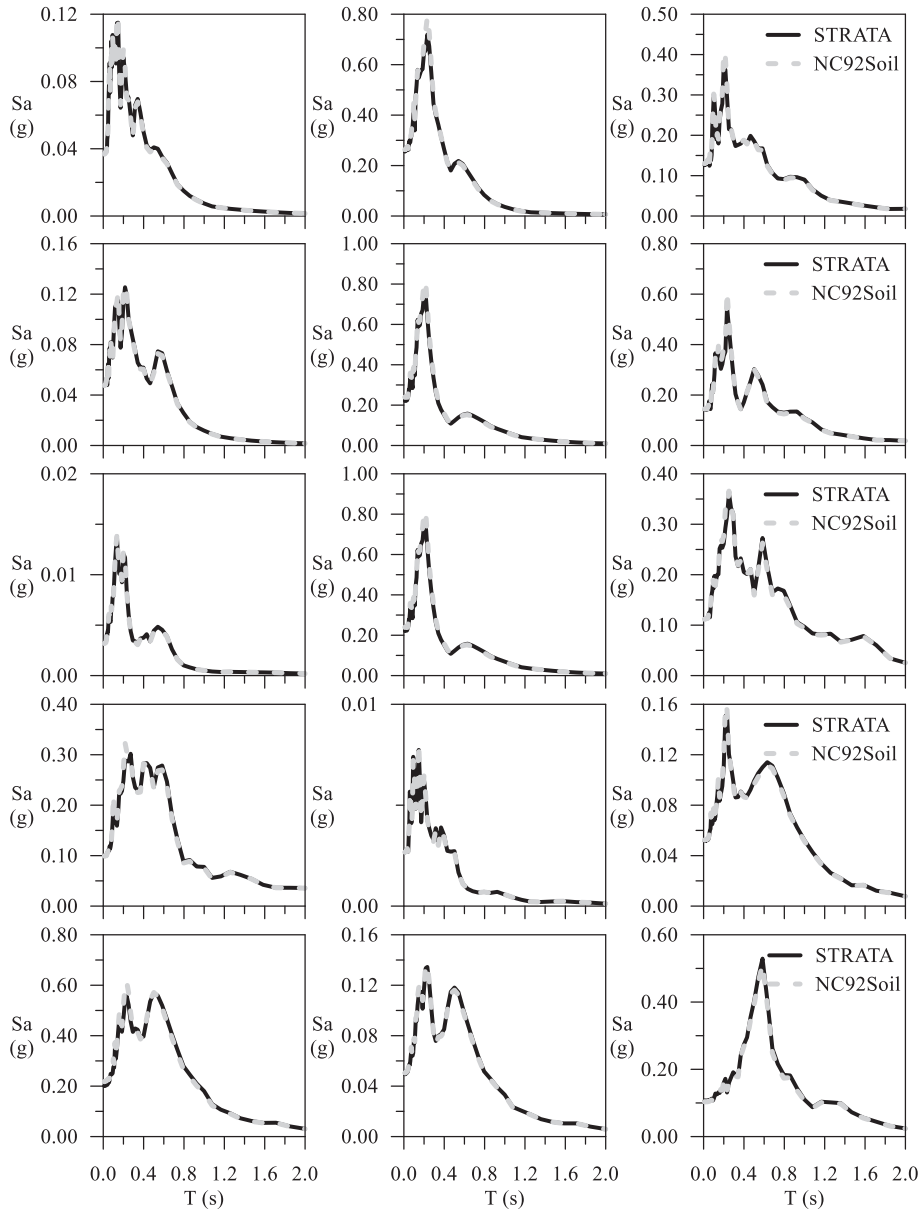

Fig. A4. Free-field response spectra obtained by means of codes STRATA and NC92Soil with reference to profile #5.

database including site key-parameters and the synthetic results of the 90,000 LSSR analyses are freely available (Falcone 2023).

5. Conclusions

A new computer code, capable of performing deterministic and stochastic site response analyses over large areas, was presented. The NC92Soil code allows to perform millions of 1D numerical simulations of the local seismic site response through the well-consolidated equivalent linear approach, aimed at providing a useful support tool for the seismic risk mitigation policy and the emergency management system. In case of large, not well-characterised areas, the code allows the generation of permutated lithotype successions, as well as stochastic shear wave velocity profiles, consistent with the expected lithostratigraphic site conditions, by managing the soil data available for the area by means of a Monte Carlo approach. In addition, the proposed code provides results of local seismic site response analyses not only in terms of acceleration time histories, Fourier spectra and response spectra, but also in terms of synthetic parameters, describing the geometrical and mechanical properties of soil columns and the amplification factors. This kind of outcomes can be straightforwardly adopted for microzonation studies, requiring the construction of Amplification Factors maps in accordance with the Italian seismic microzonation guidelines.

First of all, the NC92Soil code performance in executing LSSR analyses was validated by comparing the results with the well-consolidated STRATA code, confirming a perfect agreement. In addition, the capability of the code to generate stochastic shear wave velocity profiles was tested and compared to STRATA code, with reference to two target site profiles. The analysis of the results revealed a better performance of the proposed code in generating any seismic soil profile. Indeed, all the returned seismic soil profiles were consistent to the target site profiles, contrarily to STRATA profiles which were limited to the restrictions imposed to be compatible to recommendation for American sites.

As an example of the NC92Soil code potentiality, 9,000 profiles of shear wave velocity were generated, compatible with the Italian database for seismic microzonation, in order to perform 90,000 local seismic site response analyses, with the aim of identifying a correlation between amplification factors, AF, and both mean shear wave velocity in the

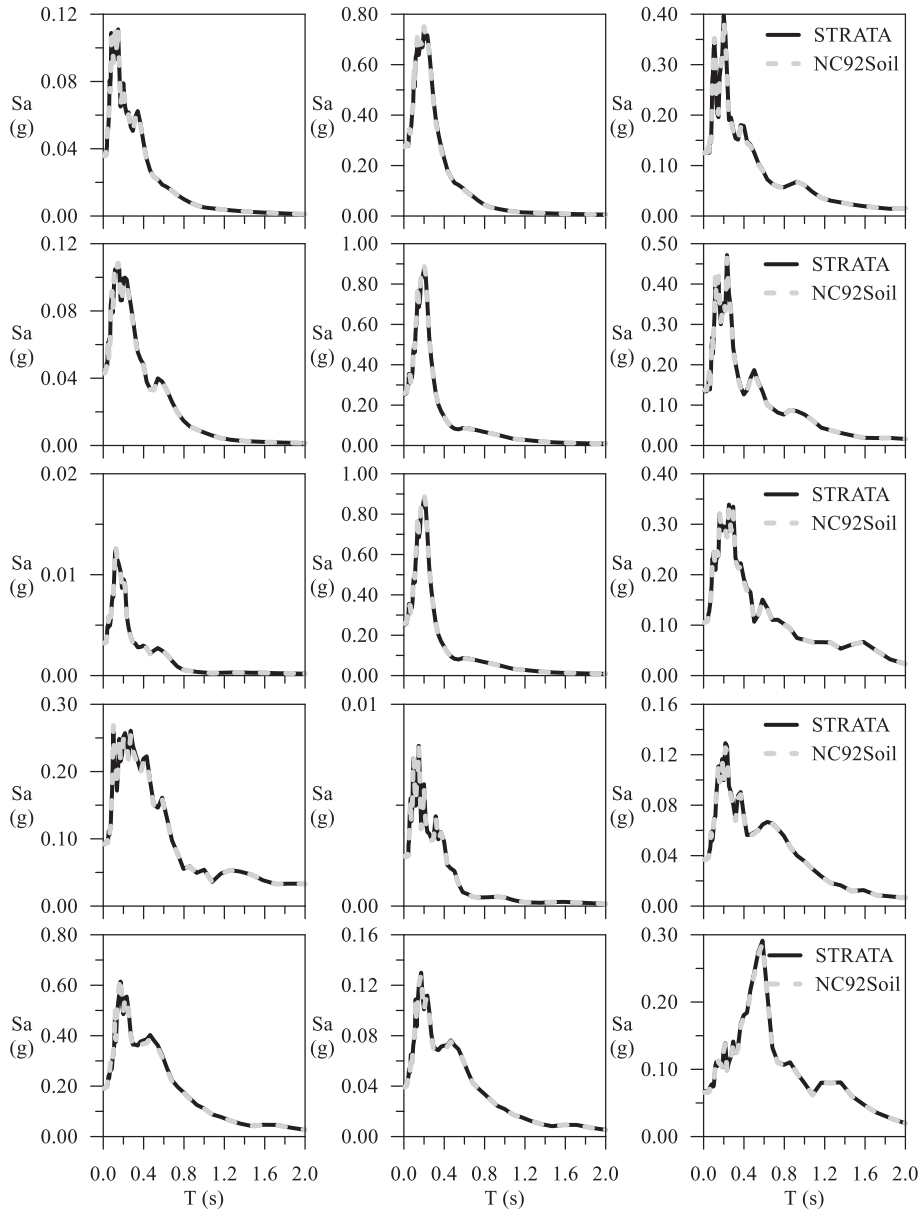

Fig. A5. Free-field response spectra obtained by means of codes STRATA and NC92Soil with reference to profile #6.

upper 30 m, V_{S30}, the fundamental frequency of the deposit, f_0, and the depth to the seismic bedrock, H_{800}.

In general, the AF-V_{S30}, AF-f_0 and AF-H_{800} trends depend on the outcropping lithotype, the peak ground acceleration of the input motion, PGA_{input}, and the interval of periods of interest. In detail, all the $AF_{0.1\text{-}0.5}$ distributions with V_{S30}, f_0 or H_{800} present a bell-shaped curve, which are slightly affected by the outcropping lithotype, while the PGA intensity of the input motions influences the value of either V_{S30} or f_0 at which the amplification factor is maximum. Conversely, the $AF_{0.7\text{-}1.1}$ distributions are strongly dependent on the PGA_{input}, as well as on the type of the outcropping soil layer. Indeed, $AF_{0.7\text{-}1.1}$ assume an increasing trend for decreasing values of V_{S30}, f_0 or increasing values of H_{800} for PGA < 0.1 g and a bell-shaped trend for PGA > 0.1 g. Moreover, the higher the PGA of the input motion the lower the AF peak value.

It is worth noting that the AF-V_{S30}, AF-f_0 and AF-H_{800} trends are illustrated in this study with the aim of showing some possible results that might be retrieved by the proposed code. Moreover, all the database of outputs (i.e., key-parameters of deposit as shallow lithotype and V_{S30} and synthetic output as the AFs) can be considered as a valuable database for the application of other approaches (e.g., machine learning among others). Future developments of the proposed code should provide:

- detailed output at different depth with a unique running of the code;
- profile of results with depth (PGA-z, PGV-z among others being PGV the peak ground velocity);
- the possibility to consider also the input motion applied at the interface between deposit and seismic bedrock (i.e., inside condition at the base of the numerical model) rather than at the outcropping bedrock;
- parallel computing option to improve the code performance in terms of required time to complete analyses.

CRediT authorship contribution statement

Gianluca Acunzo: Conceptualization, Methodology, Software, Validation, Formal analysis, Resources, Writing – original draft, Writing – review & editing, Supervision. **Gaetano Falcone:** Conceptualization,

Methodology, Validation, Formal analysis, Resources, Writing – original draft, Writing – review & editing, Visualization, Supervision. **Annamaria di Lernia:** Validation, Formal analysis, Writing – review & editing, Visualization, Supervision. **Federico Mori:** Conceptualization, Methodology, Writing – review & editing. **Amerigo Mendicelli:** Conceptualization, Methodology, Writing – review & editing. **Giuseppe Naso:** Conceptualization, Methodology, Resources, Writing – review & editing, Supervision, Project administration, Funding acquisition. **Dario Albarello:** Conceptualization, Methodology, Supervision, Writing – review & editing. **Massimiliano Moscatelli:** Conceptualization, Methodology, Resources, Writing – review & editing, Supervision, Project administration, Funding acquisition.

Declaration of competing interest

The authors declare that they have no known competing financial interests or personal relationships that could have appeared to influence the work reported in this paper.

Data availability

Data will be made available on request.

Acknowledgments

This research was supported by the Italian Department for Civil Protection of the Presidency of Council of Ministers within the "Contratto concernente l'affidamento di servizi per il programma per il supporto al rafforzamento della Governance in materia di riduzione del rischio sismico e vulcanico ai fini di protezione civile nell'ambito del PON Governance e Capacità Istituzionale 2014–2020 - CIG6980737E65". Authors would like to thank Fabrizio Bramerini, Sergio Castenetto, Antonella Gorini and Daniele Spina for the useful discussions. The corresponding author is grateful for the financial support provided by the European Union - Next Generation EU, in the framework of the _GRINS -Growing Resilient, INclusive and Sustainable project (GRINS PE00000018 - CUP E63C22002140007). The views and opinions expressed are solely those of the authors and do not necessarily reflect those of the European Union, nor can the European Union be held responsible for them.

Appendix A

Figs. A1–A5 show the results of the local seismic site response analyses based on STRATA and NC92soil codes with reference to the site profiles from #2 to #6 sketched in Fig. 3 of the manuscript. The NC92soil results are consistent with STRATA ones as expected.

References

Abate, G., Caruso, C., Massimino, M.R., Maugeri, M., 2007. Validation of a new soil constitutive model for cyclic loading by fem analysis. In: Solid Mechanics and its Applications. Springer Verlag, pp. 759–768.

Acunzo, 2023. NC92Soil. GitHub. https://github.com/giaacunzo/NC92Soil.git.

Akkar, S., Sandıkkaya, M.A., Bommer, J.J., 2014. Empirical ground-motion models for point- and extended-source crustal earthquake scenarios in Europe and the Middle East. Bull. Earthq. Eng. 12, 359–387. https://doi.org/10.1007/s10518-013-9461-4.

Amorosi, A., Boldini, D., Falcone, G., 2014. Numerical prediction of tunnel performance during centrifuge dynamic tests. Acta Geotech. 9, 581–596. https://doi.org/10.1007/s11440-013-0295-7.

Bardet, J.P., Ichii, K., Lin, C.H., 2000. EERA: A computer program for equivalent-linear earthquake site response analyses of layered soil deposits. Manual.

Bindi, D., Massa, M., Luzi, L., et al., 2014. Pan-European ground-motion prediction equations for the average horizontal component of PGA, PGV, and 5%-damped PSA at spectral periods up to 3.0 s using the RESORCE dataset. Bull. Earthq. Eng. 12, 391–430. https://doi.org/10.1007/s10518-013-9525-5.

Chiaradonna, A., 2022. Defining the boundary conditions for seismic response analysis—a practical review of some widely-used codes. Geosciences (Switzerland) 12, 83. https://doi.org/10.3390/GEOSCIENCES12020083/S1.

Chi-Miranda, M.A., Montejo, L.A., 2017. A numerical comparison of random vibration theory and time histories based methods for equivalent-linear site response analyses. Int. J. Geo-Eng. 8, 1–17. https://doi.org/10.1186/s40703-017-0059-6.

D'Amico, M., Felicetta, C., Russo, E., et al., 2020. Italian Accelerometric Archive v 3.1. Istituto Nazionale di Geofisica e Vulcanologia, Dipartimento della Protezione Civile Nazionale. 10.13127/itaca.3.1.

Dafalias, Y.F., Taiebat, M., 2016. SANISAND-Z: zero elastic range sand plasticity model. Géotechnique 66, 999–1013. https://doi.org/10.1680/JGEOT.15.P.271.

De Risi, R., Penna, A., Simonelli, A.L., 2019. Seismic risk at urban scale: the role of site response analysis. Soil Dyn. Earthq. Eng. 123, 320–336. https://doi.org/10.1016/j.soildyn.2019.04.011.

di Lernia, A., Buono, C., Elia, G., 2023. Evaluation of seismic site effects in a real slope through 2D FE numerical analyses. Conference proceedings of the 9th ECCOMAS Thematic Conference on Computational Methods in Structural Dynamics and Earthquake Engineering - COMPDYN2023. Athens, Greece, 12th-14th June 2023.

DPC, 2018. Commissione tecnica per il supporto e monitoraggio degli studi di Microzonazione Sismica. www.webms.it. Accessed 21 Oct 2022.

Elia, G., Rouainia, M., 2016. Investigating the cyclic behaviour of clays using a kinematic hardening soil model. Soil Dyn. Earthq. Eng. 88, 399–411. https://doi.org/10.1016/J.SOILDYN.2016.06.014.

Elia, G., Rouainia, M., Di Lernia, A., D'Oria, A.F., 2021. Assessment of damping predicted by kinematic hardening soil models during strong motions. Géotech. Lett. 11 (48–55) https://doi.org/10.1680/JGELE.20.00078.

Fabozzi, S., Catalano, S., Falcone, G., et al., 2020. Stochastic approach to study the site response in presence of shear wave velocity inversion: Application to seismic microzonation studies in Italy. Eng. Geol. 280, 105914 https://doi.org/10.1016/j.enggeo.2020.105914.

Falcone, G., 2023. LSSR data_1 NC92Soil. Mendeley Data 1. https://doi.org/10.17632/jvv59sjj8y.1.

Falcone, G., Boldini, D., Amorosi, A., 2018. Site response analysis of an urban area: A multi-dimensional and non-linear approach. Soil Dyn. Earthq. Eng. 109, 33–45. https://doi.org/10.1016/J.SOILDYN.2018.02.026.

Falcone, G., Boldini, D., Martelli, L., Amorosi, A., 2020a. Quantifying local seismic amplification from regional charts and site specific numerical analyses: a case study. Bull. Earthq. Eng. 18, 77–107. https://doi.org/10.1007/s10518-019-00719-9.

Falcone, G., Mendicelli, A., Mori, F., et al., 2020b. A simplified analysis of the total seismic hazard in Italy. Eng. Geol. 267, 105511 https://doi.org/10.1016/J.ENGGEO.2020.105511.

Falcone, G., Acunzo, G., Mendicelli, A., et al., 2021. Seismic amplification maps of Italy based on site-specific microzonation dataset and one-dimensional numerical approach. Eng. Geol. 289, 106170 https://doi.org/10.1016/j.enggeo.2021.106170.

Galli, P., Peronace, E., 2014. New paleoseismic data from the Irpinia Fault. A different seismogenic perspective for southern Apennines (Italy). Earth Sci. Rev. 136, 175–201. https://doi.org/10.1016/J.EARSCIREV.2014.05.013.

Gazetas, G., 1982. Vibrational characteristics of soil deposits with variable wave velocity. Int. J. Numer. Anal. Meth. Geomech. 6, 1–20. https://doi.org/10.1002/nag.1610060103.

Giallini, S., Pizzi, A., Pagliaroli, A., et al., 2020. Evaluation of complex site effects through experimental methods and numerical modelling: The case history of Arquata del Tronto, central Italy. Eng. Geol. 272, 105646 https://doi.org/10.1016/j.enggeo.2020.105646.

Griffiths, S.C., Cox, B.R., Rathje, E.M., Teague, D.P., 2016. Mapping dispersion misfit and uncertainty in Vs profiles to variability in site response estimates. J. Geotech. Geoenviron. Eng. 142 https://doi.org/10.1061/(ASCE)GT.1943-5606.0001553.

Guzel, Y., Rouainia, M., Elia, G., 2020. Effect of soil variability on nonlinear site response predictions: Application to the Lotung site. Comput. Geotech. 121, 103444 https://doi.org/10.1016/J.COMPGEO.2020.103444.

Hailemikael, S., Amoroso, S., Gaudiosi, I., 2020. Guest editorial: seismic microzonation of Central Italy following the 2016–2017 seismic sequence. Bull. Earthq. Eng. 18, 5415–5422.

Huber, M., Marconi, F., Moscatelli, M., 2015. Risk-based characterisation of an urban building site. Georisk 9, 49–56. https://doi.org/10.1080/17499518.2015.1015574.

Iwahashi, J., Kamiya, I., Matsuoka, M., Yamazaki, D., 2018. Global terrain classification using 280 m DEMs: segmentation, clustering, and reclassification. Prog. Earth Planet Sci. 5, 1. https://doi.org/10.1186/s40645-017-0157-2.

Kolli, M.K., Bora, S.S., 2021. On the use of duration in random vibration theory (RVT) based ground motion prediction: a comparative study. Bull. Earthq. Eng. 1–21 https://doi.org/10.1007/s10518-021-01052-w.

Kottke, A.R., Wang, X., Rathje, E.M., 2013. Technical Manual for Strata.

Kottke, A.R., Rathje, E.M., 2013. Comparison of time series and random-vibration theory site-response methods. Bull. Seismol. Soc. Am. 103, 2111–2127. https://doi.org/10.1785/0120120254.

Lo Presti, D.C., Lai, C.G., Puci, I., 2006. ONDA: computer code for nonlinear seismic response analyses of soil deposits. J. Geotech. Geoenviron. Eng. 132, 223–236. https://doi.org/10.1061/(asce)1090-0241(2006)132:2(223).

Makra, K., Chávez-García, F.J., 2016. Site effects in 3D basins using 1D and 2D models: an evaluation of the differences based on simulations of the seismic response of Euroseistest. Bull. Earthq. Eng. 14, 1177–1194. https://doi.org/10.1007/s10518-015-9862-7.

Makra, K., Chávez-García, F.J., Raptakis, D., Pitilakis, K., 2005. Parametric analysis of the seismic response of a 2D sedimentary valley: Implications for code implementations of complex site effects. Soil Dyn. Earthq. Eng. 25, 303–315. https://doi.org/10.1016/j.soildyn.2005.02.003.

Mendicelli, A., Falcone, G., Acunzo, G., et al., 2022. Italian seismic amplification factors for peak ground acceleration and peak ground velocity. J. Maps 1–11. https://doi.org/10.1080/17445647.2022.2101947.

Moczo, P., Kristek, J., Bard, P.Y., et al., 2018. Key structural parameters affecting earthquake ground motion in 2D and 3D sedimentary structures. Bull. Earthq. Eng. 16, 2421–2450. https://doi.org/10.1007/s10518-018-0345-5.

Mori, F., Gena, A., Mendicelli, A., et al., 2020a. Seismic emergency system evaluation: The role of seismic hazard and local effects. Eng. Geol. 270, 105587 https://doi.org/10.1016/j.enggeo.2020.105587.

Mori, F., Mendicelli, A., Moscatelli, M., et al., 2020b. A new Vs30 map for Italy based on the seismic microzonation dataset. Eng. Geol. 275, 105745 https://doi.org/10.1016/j.enggeo.2020.105745.

Moscatelli, M., Albarello, D., Scarascia Mugnozza, G., Dolce, M., 2020. The Italian approach to seismic microzonation. Bull. Earthq. Eng. 18, 5425–5440. https://doi.org/10.1007/s10518-020-00856-6.

Nikolopoulos, D., Mascandola, C., Lanzano, G., Pacor, F., 2022. Consistency check of ITACAext, the Flatfile of the Italian accelerometric archive. Geosciences 12, 334. https://doi.org/10.3390/GEOSCIENCES12090334.

Pagliaroli, A., Moscatelli, M., Raspa, G., Naso, G., 2014. Seismic microzonation of the central archaeological area of Rome: results and uncertainties. Bull. Earthq. Eng. 12, 1405–1428. https://doi.org/10.1007/s10518-013-9480-1.

Rathje, E.M., Ozbey, M.C., 2006. Site-Specific validation of random vibration theory-based seismic site response analysis. J. Geotech. Geoenviron. Eng. 132, 911–922. https://doi.org/10.1061/(ASCE)1090-0241(2006)132:7(911).

Rathje, E.M., Kottke, A.R., Trent, W.L., 2010. Influence of input motion and site property variabilities on seismic site response analysis. J. Geotech. Geoenviron. Eng. 136, 607–619. https://doi.org/10.1061/(ASCE)GT.1943-5606.0000255.

Régnier, J., Bonilla, L., Bard, P., et al., 2016. International benchmark on numerical simulations for 1D, nonlinear site response (PRENOLIN): verification phase based on canonical cases. Bull. Seismol. Soc. Am. 106, 2112–2135. https://doi.org/10.1785/0120150284.

Régnier, J., Bonilla, L., Bard, P., et al., 2018. PRENOLIN: International Benchmark on 1D Nonlinear Site-Response Analysis—Validation Phase Exercise. Bull. Seismol. Soc. Am. 108, 876–900. https://doi.org/10.1785/0120170210.

Romagnoli, G., Tarquini, E., Porchia, A., et al., 2022. Constraints for the Vs profiles from engineering-geological qualitative characterization of shallow subsoil in seismic microzonation studies. Soil Dyn. Earthq. Eng. 161, 107347 https://doi.org/10.1016/J.SOILDYN.2022.107347.

Santucci de Magistris, F., D'Onofrio, A., Penna, A., et al., 2014. Lessons learned from two case histories of seismic microzonation in Italy. Nat. Hazards 74, 2005–2035. https://doi.org/10.1007/s11069-014-1281-6.

Silvestri, F., Forte, G., Calvello, M., 2019. Multi-level approach for zonation of seismic slope stability: Experiences and perspectives in Italy. In: Landslides and Engineered Slopes. Theory and Practice. CRC Press, Experience, pp. 101–118.

Stucchi, M., Meletti, C., Montaldo, V., et al., 2011. Seismic Hazard Assessment (2003–2009) for the Italian Building Code. Bull. Seismol. Soc. Am. 101, 1885–1911. https://doi.org/10.1785/0120100130.

Toro, G.R., 1995. Probabilistic models of site velocity profiles for generic and site-specific ground-motion amplification studies. New York.

Tropeano, G., Chiaradonna, A., D'Onofrio, A., Silvestri, F., 2016. An innovative computer code for 1D seismic response analysis including shear strength of soils. Géotechnique 66, 95–105. https://doi.org/10.1680/jgeot.SIP.15.P.017.

Tropeano, G., Silvestri, F., Ausilio, E., 2017. An uncoupled procedure for performance assessment of slopes in seismic conditions. Bull. Earthq. Eng. 15, 3611–3637. https://doi.org/10.1007/s10518-017-0113-y.

Varone, C., Carbone, G., Baris, A., et al., 2023. PERL: a dataset of geotechnical, geophysical, and hydrogeological parameters for earthquake-induced hazards assessment in Terre del Reno (Emilia-Romagna, Italy). Nat. Hazards Earth Syst. Sci. 23, 1371–1382. https://doi.org/10.5194/NHESS-23-1371-2023.

Vucetic, M., Dobry, R., 1991. Effect of Soil Plasticity on Cyclic Response. J. Geotech. Eng. 117, 89–107. https://doi.org/10.1061/(ASCE)0733-9410(1991)117:1(89).

Working Group S, 2015. Guidelines for Seismic Microzonation (English version). Rome.

Zalachoris, G., Rathje, E.M., 2015. Evaluation of one-dimensional site response techniques using borehole arrays. J. Geotech. Geoenviron. Eng. 141 https://doi.org/10.1061/(ASCE)GT.1943-5606.0001366.

Zhu, C., Pilz, M., Cotton, F., 2020. Which is a better proxy, site period or depth to bedrock, in modelling linear site response in addition to the average shear-wave velocity? Bull. Earthq. Eng. 18, 797–820. https://doi.org/10.1007/s10518-019-00738-6.